

Plasma astrophysical considerations on geometrical structure of point particles

M. Honda

Plasma Astrophysics Laboratory, Institute for Global Science, Mie, Japan

February 12, 2021

Abstract. A unific helical field as geometric structure in an internal space is proposed which has the ability to serve attributes inherent to point particles. Transition between our observational space and the warped infinitesimal space is considered in an operational fashion. It is seen, that rotational eigenvalue equation satisfied by the vector field equivalent to Gromeka-Beltrami flow familiar to plasma astrophysics provides a spatio-unifier that sustains complex orthogonal coupling between rotational, internal coordinate space and angular momentum space. Self-consistent normalization of the rotational coordinate owing to the unifier is compared to renormalization of quantum electrodynamics. A numerical value comparable to the electromagnetic coupling constant in the nonrelativistic limit is derived from theoretical analysis involving the rotational eigenvalue that charged leptons should internally refer to. It is found that chiral asymmetry of the helical eigenflows can be reflected in electroweak symmetry breaking. This study might provide a key to settle geometrical problem of preceding theories accommodated by extra-dimensions of space.

Keywords: leptons, gauge fields, infinitesimal region, Gromeka-Beltrami flow, helical structure, chiral asymmetry, coordinate self-renormalization

1. Introduction

Reducing elements of matters has continuously been the cutting edge issue on natural philosophy and physics, and the quest is currently directed toward revealing structure of quarks and leptons. Let us focus on the electron that can be isolated stably. As the matter now stands, one has none of observational evidence of the element-divided substructure; upper limit of the radius is reported 10^{-20} cm [1]. Unless the electron is made out of any solid ingredient, we would have no choice but to consider that the electric charge e and spin $1/2$ as the observed attributes reflect structure of another space expanded somewhere in a virtually infinitesimal region. From the observational fact that magnetic monopole has not yet been discovered [2], it is anticipated, that the mechanism that generates magnetic dipole moment coupled with the spin angular momentum $\hbar/2$, where $\hbar = h/2\pi$ (h is the Planck

constant) [3], is in an asymmetric relation with the mechanism that generates e , while being in a complementary relation with it.

When we embark on elucidation of the structure that engenders those attributes, the worthwhile first step is to find the analogy in structure of nucleon having its size as large as the classical electron radius. The nucleon is constantly emitting and absorbing π -meson, to have the boson cloud (see, e.g. [4]). We recall that this picture is similar to the one of electron in quantum electrodynamics (QED) such that virtual photon dresses it. As for orbital angular momentum \mathbf{L} , the pion cloud is required to have the eigenvalue of $l = 1$; this means that the pion is really rotating on an orbit. In regard to the connection with the spin angular momentum of electron, no longer in doubt is validity of imposing the commutation relation equivalent to that for the operator of $\mathbf{L} = \mathbf{R} \times \mathbf{P}$, on \mathbf{S} [3], where the notations are standard. Accordingly, it would be a decent attempt to envisage, for generation principle of \mathbf{S} , a rotational coordinate of the space expanded in the infinitesimal region of $|\mathbf{R}| \rightarrow 0$. However, primitive question of like what coordinate must be rotated has hitherto remained unanswered.

It is not totally absurd to look for, further in macroscopic objects, a clue to the puzzle, since in fact the asymmetry of the electromagnetic attributes is being cast to predominance of magnetic fields over cosmological scales [5, 6]. It is plasma physics that accounts for the dynamics of many-body system of charged particles interacting with classical electromagnetic fields. In the context, it will be better to seek out, in magnetohydrodynamical features of plasma, an intuitive image for the \mathbf{S} generation. Now, we closer look at the astrophysical jets, which are launched from active galactic nuclei including black holes, to extend up to million light years. Intriguingly, in the jets we often recognize signatures of helical motion as well as helical structure of magnetic field [7]. Such structure could appear as a result of the turbulent process of plasmas, in which the magnetic field configuration with the minimum energy is self-organized under conservation of the magnetic helicity [8, 9]. Actually, helical magnetic field structure observed in, for example, interplanetary magnetic clouds [10] and plasma ejecta in the solar corona [11] has been interpreted as this kind of relaxed state. Therefore, the structure formation is supposed a universal magnetohydrodynamical phenomenon. In this aspect, reminding that the pion could be regarded as the lowest energy excitation state in vacuum, we conjecture that the helical structure might reflect the geometrical structure that generates the rotational, internal coordinates connecting to \mathbf{S} . In regard to this, comparing the galactic nucleus to one neutron,

we consider the nuclear reaction of $n^0 \longrightarrow p^+ + \pi^-$, where p^+ and π^- are proton and π^- -meson, respectively. We then make a spinning black hole [12] and accretion disk [13] correspond, respectively, to p^+ and its π^- cloud. This leads to correspondence between a bipolar jet and lepton pair emitted in decay of π^- . Altogether, the activity of galactic nuclei is seen as though visual projection of β -decay. In particular, the lepton–jet correspondence subject to the aforementioned conjecture seems to signify that the structure in the infinitesimal space and outer space is described by common geometry. This speculation is original motivation of the present study.

The crucial thing, that divergence difficulty incidental to electron can be successfully removed by the well-defined renormalization of QED, implies latency of a fundamental operation related to transition to the infinitesimal space. If nature is essentially inventive, geometry of the space should be able to provide, in a self-consistent manner, the physical meaning of charge renormalization, which has been obscure [14]. Meanwhile, polarization picture of QED vacuum itself suggests that one could by no means reach generation principle of e within the theoretical framework that postulates vacuum dielectric (and magnetic) permittivity to be constant. This originates from the logical structure of gauge symmetry based on causality, such that in space-time concept, existence of photon having the speed c results necessarily from charge conservation. Put another way, the problem intrinsic is what the framework is not of background independence. By taking a hint from this impasse *per se*, a naïve attempt is made here to find out a form of the concerned operation: we anticipate slight vestige of that form in the macroscopic dielectric distribution such that phase velocity of light deviates from c . When contrasted with the magnetohydrodynamical analog of spin generation, the guideline is obtained in which one should also have an insight into collective phenomena of plasma as dielectric medium, particularly, dispersion of light propagating through the plasma.

Of course, it is impossible from plasma physics to literally derive the microscopic mechanics that assigns “point” the intrinsic attributes. However, when specific description of plasmas as the dielectric and magnetofluid is appropriately generalized and/or abstracted, we may get a fortuitous chance to encounter an essential mechanism engendering e and h . The hope is that this breaks a stalemate in particle physics. If the fundamental framework found out provide radical representation of space-time independently of background, it would encompass generation mechanism of the fine-structure constant (including c) $e^2/2hc =: \alpha$ [15], and its relation to the other interactions. Mechanics in the infinitesimal space

should describe observable phenomena of particles and fields in the infinite limit. Thus, priority task is to specify the space-transformation operation responsible for the reproducibility.

In the present paper, by virtue of the heuristic way, I explore the geometrical structure of point-like particles including the electron. Making reference to plasma dielectric dispersion theory, I propose a convenient form of the transformation that describes transition to the space warped in the infinitesimal region. I show that the space is the cylindrical one, which is, in association with symmetry breaking, spanned by a unific rotational field equivalent to Gromeka-Beltrami vector flow [16]. The field obeys the rotational eigenvalue equation, which is found to describe generation of angular momentum space orthogonal to coordinate space. We figure out that spin precession of electron is appearance of the generation mechanism of time as one degree of freedom, which owes to complementation of those isotopic spaces under the rotation. The electromagnetic coupling refers to a left-handed rotational eigenmode, and this property is linked to parity violation in the β -decay [17, 18]. This eigenmode regulates helical structure of the rotational field. The related geometry is the same as that to describe the helical structure of the relaxed plasma, whereby we reconfirm significance as to the lepton–astrophysical jet correspondence. It is noticed here that the geometrical theory is distinct from the previous morphology in [19], which was built within, basically, an ordinary macroscopic framework of plasma physics.

This paper is organized as follows: Section 2 is devoted to preparation for expanding major geometrical part of the theory. We revisit the optical dispersion of plasma (section 2.1), to arrange a rule of the wavenumber transformation of light accompanying plasma nonuniformity (section 2.2). Taking the abstracted form into account, proposed is the spatial transformation to the infinitesimal space of particles (section 2.3). To test its applicability to generation of particle fields, in section 3 we call quark condensate, as it resembles the massive photon state owing to harmonic oscillator behavior of plasma electrons. We reproduce familiar potential inside [20] (section 3.1) and outside meson [21] (section 3.2), clarifying a signature of the cylindrical space expanded in the infinitesimal region. In section 4, I provide a module representation of β -decay products and the related gauge bosons. Considering internal coupling of electron with virtual photon, the rotational eigenvalue equation is proposed which governs vector field spanned in the cylindrical space (section 4.1). The equation is solved as a boundary value problem, to yield the eigenstates that the lepton pairs should

refer to (section 4.2). The eigenmode property is compared with the CP symmetry (section 4.3). The other eigenmode representing the weak is also noted (section 4.4). In section 5, I address major issues concerning observation of the rotational field of a single electron. We focus on constructing the geometrical mechanics that sets up \mathbf{R}^3 rotational coordinate of electron cyclotron motion (section 5.1). From the rotational eigenvalue equation governing the field, we derive a mathematical symbol that generates the spin precession (section 5.2). Then, we attempt to make correspondence between the mechanical sequence and the QED renormalization (section 5.3). For the sake of reinforcing the theory, section 6 is added wherein its compatibility with foundation of the standard model is examined. First, I provide a plausible explanation of how fractional charge of quark [22] could appear as reconciled with the α -generation (section 6.1). Second, I argue the compatibility with the established framework of vacuum [23] (section 6.2), and third, provide a notion of rotational eigenmode coupling responsible for the electroweak coupling [24, 25, 26] (section 6.3). Last section 7 is devoted to concluding remarks.

2. Abelian plasma analogy to a feasible form of spatial transformation

It is known, that classical field theory appropriately provides physical elements to understand the quantum field theory (e.g. [27]) that any modern approach to theories of fundamental interactions is based on. In what follows, collective harmonic oscillator behavior is reconsidered as available for making suitable analogy to the novel transformation that is referred later in the geometrical theory (compatible with the quantum field theory) away from the classical field theory.

2.1. Massive photon picture for plasma dielectric response, revisited

We begin with considering a discharged gas distributed in vacuum, which comprises freely moving electrons and the charge compensating ions. Light propagating through it induces currents carried mainly by electrons having the small inertia, whereupon this effect is fed back to the light. The interaction gives rise to optical dispersion. When describing this phenomenon theoretically, one calls the Maxwell equation in vacuum, taking the free currents into account. For simplicity, provided the background ions are immovable, the current formation is considered which involves harmonic oscillation of the nonrelativistic electrons that experience a single force $-e\mathbf{E}$, where \mathbf{E} is the self-consistent electric field. In this model, one has the Klein-Gordon equation

for transverse electromagnetic fields $\Psi: \{\mathbf{E}, \mathbf{B}\}$ [28]:

$$(\partial_t^2 - c^2 \Delta) \Psi = -(ne^2/m_e)\Psi, \quad (1)$$

where $\partial_t^2 = \partial^2/\partial t^2$, $\Delta = \nabla^2$, and n and m_e are the plasma density and the electron rest mass, respectively. When assuming the plasma and plane wave to be infinitely pervading the vacuum, equation (1) immediately leads to the dispersion relation of the electromagnetic wave having its angular frequency ω and wavenumber \mathbf{k} :

$$\omega^2 = c^2 \mathbf{k}^2 + \omega_p^2, \quad (2)$$

where ω_p is the plasma frequency that satisfies $\omega_p^2 = ne^2/m_e$ [29]. For equation (2), the refractive index is given by $ck/\omega = \sqrt{1 - (\omega_p^2/\omega^2)}$, where $k = |\mathbf{k}|$. On both sides of equation (2), we multiply \hbar^2 , and introduce $E = \hbar\omega$ and $\mathbf{p} = \hbar\mathbf{k}$, respectively, as energy and momentum eigenvalue of the light quantum. Then, the relativistic relation comes out, to give [30]

$$E^2 = c^2 \mathbf{p}^2 + m^2 c^4, \quad (3)$$

where m is defined by

$$m = \hbar\omega_p/c^2, \quad (4)$$

so that it has dimension of mass. This suggests that the photons behave as if they have the mass, as similarly seen in superconductors.

It should be noted that real position vector \mathbf{R} of the harmonic oscillator, which assigns the photons m , is parallel to \mathbf{E} (resp. perpendicular to magnetic field \mathbf{B}), on account of $\mathbf{R} = (e/k_s)\mathbf{E}$ (resp. $\perp \mathbf{B}$), where $k_s = m_e\omega^2$ is equivalent to the spring constant. This means, when regarding k_s/e as an arbitrary constant Λ such that $\Lambda \rightarrow 0$ reflects $E (= \hbar\omega) \rightarrow 0$, equation (1) with the following replacement results in describing the coordinate wave that traces position of the electrons:

$$\mathbf{E} \longrightarrow \Lambda \mathbf{R}, \quad \mathbf{B} \longrightarrow i\Lambda \mathbf{R}, \quad (5)$$

where $i = \sqrt{-1}$. Equation (5) seems to expose a hidden projective form relating photons to rotational coordinate, in accordance with the intuitive image of spinning electron. Besides, a view of the coordinate wave is reminiscent of general coordinate transformation of space-time [31]. These stuffs imply that the electron will be with symmetry between photon and graviton, characterized by c , thereby, including the origin of α (see also, e.g. [32]).

2.2. Wavenumber transformation of light

2.2.1. Elementary excitation representation of a propagative massive photon The nonuniformity of plasma, which varies phase velocity of the light, is taken into consideration. For instance, as shown in figure 1(a), we set two distinct regions: high density region I specified by the plasma frequency of ω_{p1} and

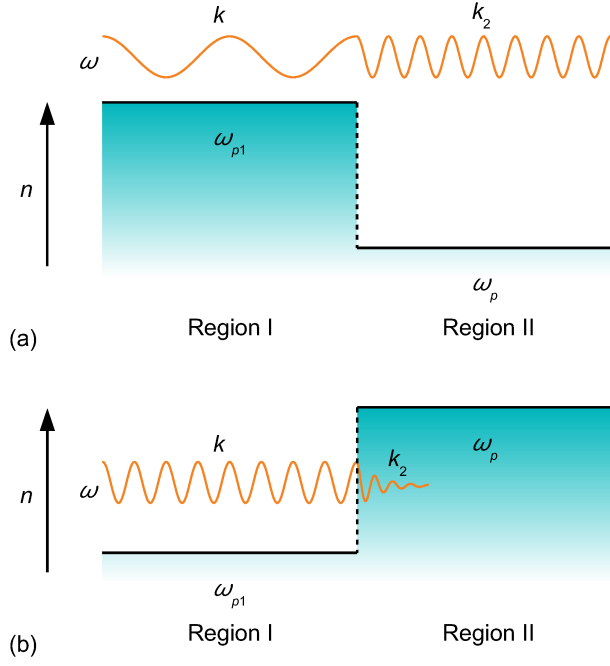


Figure 1. Schematics of the wavenumber transformation $k \rightarrow k_2$, which comes about when light (orange solid curves) propagates from plasma region I to II across the boundary (dashed lines): a surface of discontinuity of the density n (solid lines). Assuming angular frequency of the light, ω , to be invariant for the transformation, shown are the cases of $\omega_p < \omega_{p1} < \omega$ (a) and $\omega_{p1} < \omega < \omega_p$ (b), where ω_{p1} and ω_p stand for the plasma frequency of the region I and II, respectively.

low density region II by that of $\omega_p (< \omega_{p1})$ such that on an infinite boundary surface, these come in contact with one another. Monochromatic light with $\omega (> \omega_{p1})$ propagating through the region I in the direction normal to the contact surface is transmitted to the region II across the surface. Provided ω is unchanged in the entire process, the dispersion relations in the region I and II can be written as $\omega^2 = c^2 k^2 + \omega_{p1}^2$ and $\omega^2 = c^2 k_2^2 + \omega_p^2$, respectively. By combining them, we obtain, for positive real wavenumber transformation of $k \rightarrow k_2$, the factorized representation of k_2 :

$$k_2 = \sqrt{\left(k^2 + \frac{\omega_{p1}^2}{c^2}\right) \left(1 - \frac{\omega_p^2}{\omega^2}\right)}. \quad (6)$$

Note that the second factor of the right-hand side is just the refractive index: $\tilde{n} = ck_2/\omega$ in the region II.

Here, the situation is supposed in which keeping the ratio of ω_p/ω constant, $\omega \downarrow \omega_{p1}$ is taken to give $k \rightarrow 0$. Introducing definitions of $\mu = k_2|_{k=0}$, $\bar{\mu} = \sqrt{\omega_{p1}^2/c^2 + k^2}|_{k=0}$, and $\delta = \omega_p^2/\omega^2|_{\omega=\omega_{p1}}$, the wavenumber transformation can be expressed as

$$k(=0) \rightarrow \mu = \bar{\mu}\sqrt{1-\delta}. \quad (7)$$

Equation (7) can be regarded as representing creation of a propagative photon having the mass of $m = \hbar\bar{\mu}/c$.

Particularly, in the case for which $\delta \ll 1$, the phase velocity in the region II, c/\tilde{n} , is approximately given by $c(1 + \delta/2)$, so that it indicates small deviation from c . This is of the property desired in terms of a clue to the spatial transformation. Expected is relation of equation (7) with the lowest energy excitation of real particles.

It is noticed that, when comparing the massive photon to a real matter particle, we should take the group velocity of photon into consideration. The lowest energy excitation with $c^{-1}|\partial\omega/\partial k| = \beta (< 1) \rightarrow 0$ can be translated into well-separation of the kinetic energy $(\Gamma - 1)mc^2|_{\Gamma \rightarrow 1}$ from the total energy $E = \Gamma mc^2|_{\Gamma \rightarrow 1}$, where $\Gamma = (1 - \beta^2)^{-1/2}$. More specifically, this can be compared to transition from $E(\mathbf{p})/c|_{|\mathbf{p}|=0} = mc$ to the nonrelativistic momentum $\beta mc|_{\beta \rightarrow 0}$. This suggests that $\bar{\mu} = \omega(k)/c|_{k=0} = mc/\hbar$ should be replaced by $\beta mc/\hbar|_{\beta \rightarrow 0}$ with the value remaining finite.

2.2.2. Elementary excitation representation of a non-propagative massive photon The density profile is inverted with respect to the propagation direction of the light. As shown in figure 1(b), we configure low density region I with the plasma frequency of ω_{p1} and high density region II with $\omega_p (> \omega_{p1})$ such that an infinite contact surface separates them. The light with $\omega (> \omega_{p1})$ propagating through the region I normally incidents on the surface to be transmitted to the region II. Here, the situation is considered in which the transmitted light decays due to $\omega < \omega_p$. For the dispersion relations same as given above, we obtain, for $k \rightarrow k_2$, the following representation of k_2 :

$$k_2 = -i(\omega_p/c) \sqrt{1 - (\omega^2/\omega_p^2)}, \quad (8)$$

making the negative sign have the physical meaning that a damping solution has been chosen. Again keeping the ratio of ω/ω_p , $\omega \downarrow \omega_{p1}$ is taken to give $k \rightarrow 0$, and then, the wavenumber transformation can be expressed as

$$k(=0) \rightarrow \mu = -i\bar{\mu}^* \sqrt{1-\delta} =: -i\mu^*, \quad (9)$$

where $\bar{\mu}^* = \omega_p/c$, $\delta = \omega^2/\omega_p^2|_{\omega=\omega_{p1}}$, and $m^* = \hbar\bar{\mu}^*/c$, which signifies mass of non-propagative photon. Expected is relation of equation (9) with the lowest energy excitation of virtual particles.

2.3. The abstracted implementation in the spatial transformation

The wavenumber transformation of the massive photon is coupled with coordinate of the propagation direction, to generate phase transformation of Ψ between the region I and II. This feature provides heuristic analogy to the transformation between internal space of particle and \mathbf{R}^3 real space from which observer looks into it. The transformation should be related to the

generation of wavefunction of the particle, which coincides with potential expansion into \mathbf{R}^3 . We here consider a generic form of static, three-dimensional isotropic potential, $V(\xi')$, centered at coordinate origin $(X, Y, Z) = (0, 0, 0)$ in the flat \mathbf{R}^3 . Here, as a definition of the dimensionless variable, given is $\xi' = \bar{\mu}|\mathbf{R}| = \bar{\mu}R \in (0, +\infty)$. For an equipotential surface of $R = \sqrt{X^2 + Y^2 + Z^2} = \xi'/\bar{\mu}$, a circle having the dimensional radius R can be put on the equatorial plane $Z = 0$. This locus is described by the blowup:

$$\tilde{X} = \mu R \cos \theta' = \xi' \cos \theta', \quad (10a)$$

$$\tilde{Y} = \mu R \sin \theta' = \xi' \sin \theta', \quad (10b)$$

and dimensionless equation of the circle is given by

$$\tilde{X}^2 + \tilde{Y}^2 = \xi'^2. \quad (11)$$

For $V(R)$, we set a domain of definition in the region of $R \neq 0$. Introducing the minimum allowable radius of the equipotential sphere ϵ , supposed is that in the domain of $R \geq \epsilon$, $\bar{\mu}R$ indicates a well-defined real value of ξ' . On the other hand, in the domain of $R < \epsilon$ where indetermination led by $R \rightarrow 0$ essentially sets in, we require discontinuous transition from equation (11) to

$$\tilde{X}^2 + \tilde{Y}^2 = 0, \quad (12)$$

as a plausible expression of null radius, for $|\tilde{X}| \rightarrow 0$ and $|\tilde{Y}| \rightarrow 0$. Although this appears to be in contradiction with the classical Pythagorean theorem, there is a physical reasoning by which to escape from the dilemma:

We reconsider a non-propagative photon characterized by the real mass $m^* (\neq 0)$, real energy $E (< m^*c^2)$, and imaginary momentum \mathbf{p}_i . We then make the null vector transition from the virtual particle state having a real p^* that satisfies $p^{*2} = -\mathbf{p}_i^2$, into massless state:

$$(E/c)^2 + p^{*2} = (m^*c)^2 \rightarrow (E/c)^2 + p^{*2} = 0. \quad (13)$$

This is made to correspond to equation (11) \rightarrow (12). The transition of (13) with $E/c \rightarrow 0$ and $p^* \rightarrow 0$ actually allows for replacement such as $E/c \rightarrow \mathbf{p}$ and $p^* \rightarrow i\mathbf{p}$, with \mathbf{p} being a real three-dimensional vector. The massless particle having the momentum \mathbf{p} whose magnitude indicates E/c is definitely an entity observed as photon in vacuum. Hence, equation (13) accommodated by the replacement is a physically possible process as spatial transfer from the medium to the vacuum.

The singular region characterized by equation (12) is referred to as infinitesimal region. In correspondence to what observer can never jump on internal coordinate of the massless photon, \mathbf{R}^3 spanned by $V(R)$ cannot exist in the infinitesimal region due to the definition. Nevertheless, in analog of the replacement by which to access to the eigenstate of the photon, one can figure out the spatial transformation to access to

internal coordinate inherent to particles. That is, for equation (11) \rightarrow (12), the following replacement invoking a basis vector $\hat{\mathbf{x}}$ could hold:

$$\tilde{X} \sim \cos \theta' \rightarrow \hat{\mathbf{x}}, \quad \tilde{Y} \sim \sin \theta' \rightarrow i\hat{\mathbf{x}}. \quad (14)$$

When introducing the orthogonal basis vector $\hat{\mathbf{y}}$ that satisfies $\hat{\mathbf{y}} = i\hat{\mathbf{x}}$, we obtain $\tilde{Y} \rightarrow \hat{\mathbf{y}}$. As is, it turns out that equation (14) prompts leap from the real XY -plane to Wessel-Argand-Gauß (complex) plane, settling $\hat{\mathbf{x}}$ and $\hat{\mathbf{y}}$ as the axes. This plane exists in $\mathbf{r}^3 \times \mathbf{r}^3$ host space as a null complex three-dimensional space subject to $\hat{\mathbf{x}} + i\hat{\mathbf{y}} = \mathbf{0}$, sustaining orthogonality of the two \mathbf{r}^3 -real spaces. On the plane we set $\zeta = \tilde{x} + i\tilde{y}$ with \tilde{x} and \tilde{y} real, to give $(\tilde{x}, \tilde{y}) = (\xi \cos \theta, \xi \sin \theta)$ as with equations (10a) and (10b). It is a matter of finding a linear transformation of $(\theta', \xi') \rightarrow (\theta, \xi)$ responsible for $(\tilde{X}, \tilde{Y}) \rightarrow (\tilde{x}, \tilde{y})$, such as $\theta'/g_0 \rightarrow \theta$ and $\xi'/g_0 \rightarrow \xi$ with $g_0 = 2$, in consideration of the multiplicity of \mathbf{r}^3 and loop continuation of $2\pi\xi' = g_0(2\pi\xi)$. Putting $\xi = kr \in (0, \infty)$ for $\zeta \in \mathbb{C}_* \subseteq \{\tilde{z} \in \mathbb{C} \mid \tilde{z} \neq 0\}$, $\xi' \rightarrow g_0\xi$ is cast to the expression of $\bar{\mu}R (= \infty \cdot 0) \rightarrow g_0kr$, where the left-hand side (LHS) including the round bracket represents that for $R \rightarrow 0$ and $\bar{\mu} \rightarrow \infty$, $\bar{\mu}R$ is in essentially indeterminate region, manifesting extension of the number system $\mathbb{R}_* := \{\xi', -\xi'\}$. When formally introducing variable change of $g = g_0\sqrt{1 - \delta}$ with δ being a parameter, we have

$$\mu R (= \infty \cdot 0) \rightarrow gkr, \quad (15)$$

where $\mu = \bar{\mu}\sqrt{1 - \delta}$. Equations (14) and (15) can be understood as a feasible form of transformation from \mathbf{R}^3 to the infinitesimal $\mathbf{r}^3 \times \mathbf{r}^3$ space, along with $\mathbb{R}_* \cup \{\pm\infty\} \supset \{\frac{\pm\xi'}{\infty}\} = \{0\} \rightarrow \mathbb{C}_*$ or $\mathbb{R}_* \cup \{\pm 0\} \supset \{0\} \rightarrow \mathbb{C}_*$, to be involved in potential transformation of $V(\xi') \rightarrow \eta(\xi)$.

Let us now consider the inverse transition: $\mathbf{r}^3 \times \mathbf{r}^3 \rightarrow \mathbf{R}^3$ in order to get a transformation of which the output is $V(\xi')$. For the inverse of equation (14), we can read off the following replacement, invoking a basis vector $\hat{\mathbf{X}}$:

$$\tilde{x} \sim \cos \theta \rightarrow \hat{\mathbf{X}}, \quad i\tilde{y} \sim i \sin \theta \rightarrow -\hat{\mathbf{X}}. \quad (16)$$

As the inverse of equation (15) in which equation (16) is involved, a possible form is

$$kr (= 0 \cdot \infty) \rightarrow g^{-1}\mu R. \quad (17)$$

Here, the LHS including the round bracket represents that for $k \rightarrow 0$ and $r \rightarrow \infty$, kr is in essentially indeterminate region, manifesting extension of \mathbb{C}_* . Equations (16) and (17) suggest that in the infinite distance of \mathbf{r}^3 , exists \mathbf{R}^3 , along with $\mathbb{C}_* \cup \{0\} \supset \{\frac{\xi}{\pm 0}\} = \{\pm\infty\} \rightarrow \mathbb{R}_*$ or $\mathbb{C}_* \cup \{\infty\} \supset \{\pm\infty\} \rightarrow \mathbb{R}_*$. The limit of $k \rightarrow 0$, cooperating with $r \rightarrow \infty$, may be interpreted as a projection linked to the foregoing setting of $Z = 0$ in \mathbf{R}^3 .

Equation (17) appears to be of the form that enables us to make $k (= 0)$ and $\mu(\bar{\mu}, \delta)$ correspond to

those in equation (7), and $r = \infty$ to a bulk condition for the plane wave to have the diverging wavelength. As is, we also prepare $\mu(\bar{\mu}^*, \delta)$ with the factorized form same as equation (9), though $\bar{\mu}$, $\bar{\mu}^*$, and δ herein are, at this moment, regarded as the abstracted symbols. Here, we pay attention to what in equation (7) $k = 0$ was required for fixing $\bar{\mu}$, whereas in equation (9) $\bar{\mu}^*$ was free of k . Besides, since the previous δ could be handled as constant inherent to the dispersible media, the corresponding symbolic δ as well is supposed a constant inherent to elementary excitation. Taking all this into consideration, put forth is the $\mathbf{r}^3 \times \mathbf{r}^3 \rightarrow \mathbf{R}^3$ transformation related to the lowest energy excitation of real and virtual particle, respectively, as represented in the form of

$$kr [= 0^{(l)} \cdot \infty] \longrightarrow g_0^{-1} \bar{\mu} R^*, \quad (18a)$$

$$kr [= 0 \cdot \infty^{(l)}] \longrightarrow g_0^{-1} (-i\bar{\mu}^*) R^* = g_0^{-1} \bar{\mu}^* R. \quad (18b)$$

The primes in equations (18a) and (18b) denote that $k \rightarrow 0$ and $r \rightarrow \infty$ take the lead in the essential indetermination along with $\mathbb{C}_* \cup \{0\}$ and $\mathbb{C}_* \cup \{\infty\}$, respectively. The quantities $\bar{\mu}$ and $\bar{\mu}^*$ are related to observable mass m of real and virtual particle, by $\bar{\mu} = \beta mc/\hbar|_{\beta \rightarrow 0}$ and $\bar{\mu}^* = mc/\hbar$, respectively, where $\beta = c^{-1}(\partial E/\partial p)$.

Following equations (18a) and (18b), the previous indeterminate expression for $\bar{\mu}R$ should be rewritten as $\bar{\mu}R [= \infty \cdot 0^{(l)}]$. This realm would virtually postulate the smaller mass of $\bar{\mu} \ll \ell_P^{-1}$, viz., $R_S \ll \sim \ell_P$, where ℓ_P and R_S denote the Planck length and Schwarzschild radius [33], respectively.

3. Application of the transformation to bosonic system

3.1. Complex analytical consideration on quark-antiquark potential

Prior to application of the spatial transformation to a single fermion, we attempt its direct use for a quark pair as two-fermion system, in that the bosonic state involving harmonic oscillator behavior is closer to the massive photon state. At the outset, we recall the π^- -decay reaction compared to the galactic nuclear activity:

$$\pi^- \longrightarrow \begin{cases} \mu^- + \bar{\nu}_\mu, \\ e^- + \bar{\nu}_e. \end{cases} \quad (19)$$

Combining the second channel with $n^0 \longrightarrow p^+ + \pi^-$ leads to the β^- -decay expression of $n^0 \longrightarrow p^+ + e^- + \bar{\nu}_e$. Within the framework of [22], the elementary process can be expressed as $\nu_e + d \longrightarrow e^- + u$. For including β^+ -decay, we note quark and antiquark as q and \bar{q} , respectively, and lepton and antilepton as ℓ and $\bar{\ell}$, respectively, to give the generic expression:

$$q_L + (\bar{q})_R \longrightarrow \ell_L + (\bar{\ell})_R, \quad (20)$$

where the subscripts L and R denote the left- and right-handed state, respectively.

We aim at associating $k \rightarrow 0$ followed by equations (18a) and (18b), with elementary excitation of quarks. For the moment, this is intended for a $q\bar{q}$ pair whose motion is nonrelativistic so that $\beta \rightarrow 0$, though practically the limit is supposed, for heavier mesons, a good approximation. We call a basic form of the $q\bar{q}$ potential that has been confirmed for the relevant mesons: the Cornell potential

$$V(R) = C_1 R - C_{-1} R^{-1}, \quad (21)$$

with C_1 and C_{-1} real constants [20]. An attention is paid to the fact that this function satisfies the ordinary differential equation of

$$(d^2/dR^2 + R^{-1}d/dR - R^{-2})V = 0. \quad (22)$$

Let us see the bracket of equation (22) as the operator that works for V . Then, it seems as if exposing a part of the Laplacian for cylindrical coordinate system. On the other hand, equipotential surface of V is, in fact, not cylindrical. Therefore, the cylindrical system is, if any, an entity that ought to be distinguished from \mathbf{R}^3 . At this juncture, we virtually introduce \mathbf{r}^3 real space to configure the cylindrical system. Thereupon, we presume the harmonic function $\phi(\mathbf{r})$ spanned in the space, which satisfies $\Delta\phi(r, \theta, z) = 0$. Concerning the solution of the form of $\phi = \eta(r)e^{i(m\theta - kz)}$, we look at the following equation for η :

$$(d^2/dr^2 + r^{-1}d/dr - m^2/r^2 - k^2)\eta = 0. \quad (23)$$

For the bracket set to $|m| = 1$, taking $k \rightarrow 0$ compared to $\beta \rightarrow 0$, and simultaneously carrying out replacement of $r \rightarrow R$, bring about the operator of equation (22). Evidently, this procedure entails the function transformation of $\eta(r) \rightarrow V(R)$. Note here that $k \neq 0$ is necessary for ensuring $\mathbf{r}^3 \neq \mathbf{R}^3$.

In equation (23) divided by k^2 , we put $\xi = kr \in (0, \infty)$. In the general case for which m is integer, two linearly independent solutions to this equation are the modified Bessel functions of order m , denoted as $I_m(\xi)$ and $K_m(\xi)$ [in the case of $m \neq$ integer, $I_m(\xi)$ and $I_{-m}(\xi)$].[‡] Hence, $I_{\pm 1}(\xi)$ and $K_{\pm 1}(\xi)$ are in on the current issue. Their asymptotic forms for the small ξ , in which $k \rightarrow 0$ takes the lead, should be considered. Then, $k \rightarrow 0$ signifies the projection onto cylindrical base. The scalar function ϕ as linear combination of the asymptotic forms, $\phi(k \rightarrow 0)$, constitutes a complex function, which is denoted by $w = f(\zeta)$. Here, $\zeta = \xi e^{i\theta}$ and $(\xi \cos \theta, \xi \sin \theta) = (\tilde{x}, \tilde{y})$, along the notation in section 2.3.

Letting $u(\xi, \theta)$ and $v(\xi, \theta)$ be real functions, we postulate the complex function of $w = u + iv$ to be

[‡] Notation of special functions follows that in [34] throughout.

analytic. Then, u and v satisfy the Cauchy-Riemann equation of

$$\partial u/\partial \xi = \xi^{-1} \partial v/\partial \theta, \quad \xi^{-1} \partial u/\partial \theta = -\partial v/\partial \xi, \quad (24)$$

to be the harmonic conjugates on the $\tilde{x}\tilde{y}$ -plane. The function $w = \phi(k \rightarrow 0)$ that satisfies equation (24) can be written as

$$\lim_{k \rightarrow 0} \left[c_1 I_1(\xi) e^{i(\theta - kz)} - c_{-1} K_{-1}(\xi) e^{i(-\theta - kz)} \right], \quad (25)$$

where c_1 and c_{-1} are constants. It is found that $\mathbf{r}^3 \times \mathbf{r}^3$ spaces are required for spanning the two modes of $m = \pm 1$, to be intertwined via the complex plane. We have

$$u = \left(\frac{c_1}{2} \xi - c_{-1} \frac{1}{\xi} \right) \cos \theta, \quad v = \left(\frac{c_1}{2} \xi + c_{-1} \frac{1}{\xi} \right) \sin \theta. \quad (26)$$

Here, the variable ξ , which has a non-zero but small value due primarily to $k \rightarrow 0$, is expressed as $kr [= 0^{(\prime)} \cdot \infty]$, along with equation (18a).

Of importance is to clarify the domain of ξ allowed for equation (26), that is, the upper limit of ξ by which $r \rightarrow \infty$ is well constrained. The $f(\zeta)$ provides the following form of linear map from the complex plane ζ to w :

$$w = (c_1/2) \zeta - c_{-1} \zeta^{-1}. \quad (27)$$

With respect to magnitude of $|\zeta| = \xi = kr$, the transformation $f: (\tilde{x}, \tilde{y}) \rightarrow (u, v)$ involves a critical value of $\tilde{k} = ka = \sqrt{2c_{-1}/c_1}$ for $r = a$. For the coordinate transformation to be bijective conformal map, $\xi < \tilde{k}$ must be satisfied, so that \tilde{k} can be regarded as the upper limit of ξ . In particular, circular rotation on $\xi = \tilde{k}$ is, in the case of $c_1 c_{-1} > 0$, transformed to oscillation on line segment of imaginary axis connecting $(u, v) = (0, -\sqrt{2c_1 c_{-1}} i)$ to $(0, \sqrt{2c_1 c_{-1}} i)$ on the w -plane. On the other hand, in the case of $c_1 c_{-1} < 0$ (including the Kutta-Joukowski transform [35]), circular rotation on $\xi = \sqrt{-2c_{-1}/c_1}$ is transformed to oscillation on line segment of real axis connecting $(-\sqrt{-2c_1 c_{-1}}, 0)$ to $(\sqrt{-2c_1 c_{-1}}, 0)$. As is, two-valuedness arises on the real axis of the w -plane. It turns out that such a finite domain prohibited for real u does not appear in the former case; therein we can set \mathbb{C}_* to as $\{\zeta \mid 0 < \xi \leq \tilde{k}\}$.

In the case for which $c_1 c_{-1} > 0$, the real function of $u = \Re(w)$ could appear as equation (21). It is natural to identify the concerned \mathbf{r}^3 cylindrical space with the \mathbf{r}^3 space that has been introduced in section 2.3. In the transformation of $\mathbf{r}^3 \times \mathbf{r}^3 \rightarrow \mathbf{R}^3$ for generation of $V(R)$, the lead by $k \rightarrow 0$ and $\mathbb{C}_* \cup \{0\}$ should be involved. Recalling equation (16), u in equation (26) could be rewritten as $\eta(\xi) \hat{\mathbf{X}}$, where η stands for real amplitude of the intertwined modes. Now, the transformation is applied to $\eta(\xi)$, of which the type is the same as equation (18a):

$$\xi := kr [= 0^{(\prime)} \cdot \infty] \longrightarrow g_0^{-1} \mu R^*. \quad (28)$$

The function of R^* generated is then found to show the form of equation (21) in the low energy region for which the Schrödinger equation is responsible. It appears that R^* with the asterisk indicates coordinate of the closed \mathbf{R}^3 -space confining colors. It is remarked that $|m| = 1$ would be responsible for magnitude of spin of gauge bosons mediating the strong force.

3.2. The Yukawa potential

If one prohibits two-valuedness on the w -plane, ξ cannot exceed \tilde{k} , as long as $k \rightarrow 0$ takes the lead. This seems to catch well up characteristic of quark confinement; its connection with the Wilson's scheme is expected [36], albeit remained unsolved. In order to move to region of larger ξ , we shall prepare $\phi(r \rightarrow \infty)$ owing to the lead of $r \rightarrow \infty$, instead of equation (25), i.e.,

$$\lim_{r \rightarrow \infty} \left[c_1 I_1(\xi) e^{i(\theta - kz)} - c_{-1} K_{-1}(\xi) e^{i(-\theta - kz)} \right]. \quad (29)$$

As for indeterminate form, given herein is $\xi := kr [= 0 \cdot \infty^{(\prime)}]$. This manifests that $k \rightarrow 0$ is taken to the extent that the large ξ is well maintained. In that region, equation (29) leads to

$$\frac{c_1 e^\xi - \pi c_{-1} e^{-\xi}}{\sqrt{2\pi\xi}} \cos \theta + i \frac{c_1 e^\xi + \pi c_{-1} e^{-\xi}}{\sqrt{2\pi\xi}} \sin \theta. \quad (30)$$

For $c_{-1}/c_1 = 1/\pi$, equation (30) can be cast to the linear combination form of

$$\begin{pmatrix} c_1 \\ \pi c_{-1} \end{pmatrix} [I_{1/2}(\xi) \cos \theta + i I_{-1/2}(\xi) \sin \theta]. \quad (31)$$

This indicates that the system spanning $\phi(r \rightarrow \infty)$ can be accommodated by $\theta \rightarrow \theta'/g_0$. As is, we again apply equation (16) to (31), for setting $\mathbb{C}_* \cup \{\infty\}$, where $\mathbb{C}_* = \{\zeta \mid \tilde{k} < \xi < \infty\}$. The resulting quantity is written as $\eta(\xi) \hat{\mathbf{X}}$ as before, and then, the function η is given by

$$\eta(\xi) = -2 \begin{pmatrix} c_1/\pi \\ c_{-1} \end{pmatrix} K_{\pm 1/2}(\xi) =: c_0 K_{\pm 1/2}. \quad (32)$$

We interpret η as virtual displacement along $\hat{\mathbf{X}}$. Then, η^2 is associated with potential energy of internal harmonic oscillation. The spatial transformation of which the type is the same as equation (18b) is applied to it. This results in yielding the energy transformation of

$$\eta^{g_0}(\xi) \longrightarrow V(R) = \mathcal{G}^2 \frac{e^{-\mu^* R}}{R}, \quad (33)$$

for $c_0^2 \rightarrow \mathcal{G}^2$ with \mathcal{G} constant.

According to asymptotic property of $K_{\pm 1}(kr) \sim K_{\pm 1/2}(kr)$ for $r \rightarrow \infty$, the product $c_0^2 K_{-1/2} K_{1/2}$ can be understood as far-field interference between K_{-1} and its counterpart K_1 . In this aspect, noticed is that the same mathematical representation appears in an

attractive interaction of plasma elements; formation and interference of dipole magnetic fields characterized by $K_{\pm 1}$ can be seen in self-organization of vortices as two-dimensional structure of plasma turbulence [37] and merging of the vortices [38]. Intermittent activity of galactic nuclei is expected to establish this kind of turbulent state [39], likely followed by transition to an energy relaxed state.

The function of $V(R)$ exposes the potential energy for strong nuclear force [21], which is proportional to pion field with spin 0. The thing that inertia of the constituent quarks is so small as to degrade nonrelativistic approximation for the motion, is thought of as reflecting the constraint on $k \rightarrow 0$, contrast to the previous constraint on $r \rightarrow \infty$. Relating to this, $\xi \gtrsim \mathcal{O}(1)$ can be reflected in the \mathbf{R}^3 region for which the Yukawa potential is allowed: $R \gtrsim 1/\bar{\mu}^* = \hbar/m_\pi c$, where m_π the observed pion mass. What $k = 0$ is, in any case, prohibited in the system subject to equation (23) suggests that quarks could never be at rest.

4. Rotational field in the cylindrical space

4.1. Coupling between gauge and matter fields

We contemplate the internal transformation of k that executes equation (20). The transformation for gauge fields is to have the form of $k \rightarrow -i\mu^*$, and this is applied to $\eta \sim I_{\pm 1}(kr)$, which must be, in $r \rightarrow \infty$, coexisting with $K_{\pm 1/2}(kr)$. Then, we have $I_{\pm 1}(kr) \rightarrow \mp i J_{\pm 1}(\mu^* r)$, where double signs correspond. As a matter of course, the equation that $\eta(\mu^* r)$ obeys is $[\mu^{*-2} \nabla_{\perp}^2 + 1] \eta = 0$, where $\mu^* \neq 0$. The function η is included in the scalar function $\phi = \eta(\mu^* r) e^{i(\pm\theta - kz)}$, which is as solution of the following equation in the cylindrical system:

$$(\Delta + k^2 + \mu^{*2}) \phi(r, \theta, z) = 0. \quad (34)$$

Here, k is newly introduced of which the value can be taken arbitrarily. Appearance of the finite k without $k \rightarrow 0$ is indicative of onset of the spatial direction $\mathbf{k}/k = \hat{\mathbf{z}}$. Especially for $k = 0$, ϕ represents single-valued amplitude of vibration of a circular membrane on z -constant slices. In the current context, regarding $\eta^{g_0}(\mu^* r)$ as the internal potential that works for $\ell\ell$ pair, it is appropriate to interpret ϕ as scalar field of the weak boson. We envisage that μ^* and $|m| = 1$ are reflected in the mass and spin, respectively, and particularly, $\mu^* \rightarrow 0$ in massless photon state.

In the region that allows for $\xi := \mu^* r [= 0 \cdot \infty^{(l)}]$, $\eta \sim \mp i J_{\pm 1}(\xi)$ can be expressed as $-i[J_{-1/2}(\xi) - J_{1/2}(\xi)]/\sqrt{2}$, where $\xi \in (0, \infty)$ in the transformed system of $|m| = 1/2$. Concerning coupling of the virtual boson with leptons, we see that modules including $J_{\mp 1/2}$ are generated by applying $k \rightarrow -i\mu$ to

the internal pion field. That is, we have $K_{\mp 1/2}(kr) \rightarrow (i\pi/2)e^{\mp i\pi/4} H_{\mp 1/2}^{(1)}(\mu r)$ for reaction (19), where

$$H_{-1/2}^{(1)} e^{-i\theta/2} = [J_{-1/2}(\mu r) + iJ_{1/2}(\mu r)] e^{-i\theta/2}, \quad (35a)$$

$$iH_{1/2}^{(1)} e^{i\theta/2} = [J_{-1/2}(\mu r) + iJ_{1/2}(\mu r)] e^{i\theta/2}, \quad (35b)$$

and the complex conjugates are

$$\left[H_{-1/2}^{(1)} \right]^* e^{i\theta/2} = [J_{-1/2}(\mu r) - iJ_{1/2}(\mu r)] e^{i\theta/2}, \quad (35c)$$

$$\left[iH_{1/2}^{(1)} \right]^* e^{-i\theta/2} = [J_{-1/2}(\mu r) - iJ_{1/2}(\mu r)] e^{-i\theta/2}, \quad (35d)$$

respectively. Here, $|m| = 1/2$ is compared to spin of leptons, and all terms should be multiplied by e^{-ikz} with k newly introduced as before. The representation with $k = 0$ is compared to rest state of them, whereas $k \neq 0$ to the moving state.

When interpreting (35a) \rightleftharpoons (35c) and (35b) \rightleftharpoons (35d) as the CP transformation operation, one could associate (35a) and (35b) with $(e^-)_{\text{L}}$ and $(\bar{\nu}_e)_{\text{R}}$, respectively, emitted in β^- -decay, and (35c) and (35d) with $(e^+)_{\text{R}}$ and $(\nu_e)_{\text{L}}$, respectively, in β^+ -decay. A solution of the s-wave radial Schrödinger equation is obtained by applying $\mu r [= 0 \cdot \infty^{(l)}] \rightarrow g_0^{-1} \bar{\mu} R$ to $[H_{-1/2}^{(1)}]^{g_0}$, that is, $(4/\pi)(e^{2i\mu r}/2\mu r) \rightarrow \sim e^{i\bar{\mu} R}/\bar{\mu} R$, where $\bar{\mu} = \beta m_e c/\hbar|_{\beta \rightarrow 0}$ stands for the observed wavenumber of nonrelativistic electron. For the coupling of the matter with gauge field, we require $\xi (= \mu^* r) = \mu r$ on the cylindrical base. Here, we redefine ϕ as a module of $\phi_{m'} J_{m'}(\xi) e^{i(m\theta - \mathbf{k}\cdot\mathbf{z})}$, where $m' = \pm m$, and $\phi_{m'}$ is constant fixed later. For $|m'| = 1/2$, noted is $J_{-1/2} \gg J_{1/2}$ for $\mu^* \rightarrow 0$. Wherein the Coulomb potential energy $V(R)$ is obtained by applying $\xi := \mu^* r [= 0^{(l)} \cdot \infty] \rightarrow g_0^{-1} \bar{\mu}^* R$ to $|\phi(m' = -1/2)|^{g_0}$, that is, $(2/\pi)\phi_{-1/2}^2/\xi \rightarrow \sim \alpha/\bar{\mu}^* R = V(R)/m_e c^2$, where $\phi_{-1/2}^2 \rightarrow \alpha$ and $\bar{\mu}^* = m_e c/\hbar$. This indetermination, led by $\mu^* \rightarrow 0$, is thus related to virtual photon state. It follows that $\phi(m' = -1/2)$ gives a possible representation of internal scalar field of the virtual photon concomitant with charged leptons.

The function of ϕ satisfies

$$(\Delta + \kappa^2) \phi = 0, \quad (36a)$$

$$\kappa^2 = \mathbf{k}^2 + \mu^{*2}, \quad (36b)$$

and equations (35a)–(35d) with $\mu r = \xi$ do likewise, each consisting of the two linearly independent solutions. Following the onset of $\hat{\mathbf{z}}$, we introduce the vector field related to ϕ as

$$\Phi(\mathbf{r}) = (\mu^*)^{-2} [\nabla \times \nabla \times (\phi \hat{\mathbf{z}}) + \kappa \nabla \times (\phi \hat{\mathbf{z}})]. \quad (37)$$

This is the solution of

$$\nabla \times \Phi = \kappa \Phi, \quad (38)$$

as far as ϕ satisfies equation (36a) [40]. Noted is that Φ of equation (38) exactly represents the Gromeka-Beltrami flow. Equation (38) can be recognized as

the rotational eigenvalue equation in \mathbf{r}^3 space, so that Φ is referred to as rotational field. It follows that, in equations (36a) and (36b), ϕ reflects eigenstates of the rotational field, and at the same time, $\kappa(k, \mu^*)$ indicates the corresponding eigenvalues. An analogy to establishment of Φ can be found in topological transition of the turbulent state of plasma that has been remarked above. There is a consensus that, when the plasma attains the energy relaxed state conserving the magnetic helicity, the magnetic field self-organized macroscopically in \mathbf{R}^3 space would take a configuration such that the vector field \mathbf{B} satisfies an equation of the same form as equation (38) [8, 9].

In the case for which m is arbitrary, analytic function of Φ is written out below; this is just generalization of the special case, $m = m' = \pm 1$, the classical field theory frequently allows for. Substituting ϕ into equation (37), one can obtain the expression of $\Phi = (\Phi_r, \Phi_\theta, \Phi_z)$, where

$$\Phi_r = i \frac{\phi_{m'}}{\mu^*} \left[\frac{m\kappa}{\xi} J_{m'}(\xi) - k \frac{dJ_{m'}(\xi)}{d\xi} \right] e^{i(m\theta - kz)}, \quad (39a)$$

$$\Phi_\theta = \frac{\phi_{m'}}{\mu^*} \left[\frac{m\kappa}{\xi} J_{m'}(\xi) - \kappa \frac{dJ_{m'}(\xi)}{d\xi} \right] e^{i(m\theta - kz)}, \quad (39b)$$

$$\Phi_z = \phi_{m'} J_{m'}(\xi) e^{i(m\theta - kz)}, \quad (39c)$$

and $\xi \in (0, \infty)$.

4.2. Eigenstates of the rotational field

The helical pattern of Φ indicating rotational and translational symmetry is characterized by m as modal number, and k . In particular, $\Phi(m = \pm 1/2, m' = \pm 1/2, k)$ can be involved in equations (35a)–(35d) via $\Phi_z = \phi$ with $\xi = \mu r$, to constitute the internal structure of spin 1/2 point particles. Regarding the expression of $|\phi(m' = -1/2)| \sim \phi_{-1/2}/\sqrt{\xi}$ led by $\mu^* \rightarrow 0$, we should set an upper limit of ξ by which $r \rightarrow \infty$ is well constrained, as we have similarly set \tilde{k} reflected in the rotating $q\bar{q}$ in \mathbf{R}^{*3} (section 3.1). This provides a domain of ξ defined for $\Phi(|m| = 1/2, m' = -1/2, k)$, making the Φ discrete. In analogy with the conducting wall condition for plasma magnetic fields that retains gauge invariance, we impose on Φ_r the cylindrical boundary condition: $\Phi_r(r = a) = 0$, which can be expressed as

$$\frac{m\kappa}{\tilde{\xi}} J_{m'}(\tilde{\xi}) - k \frac{dJ_{m'}(\tilde{\xi})}{d\tilde{\xi}} \Big|_{\tilde{\xi}=\tilde{\xi}} = 0, \quad (40)$$

where $\tilde{\xi} = \mu^* a$. Expected is that eigenfunctions of $\Phi(|m| = 1/2, k)$ and $\Phi(|m| = 1, k)$ involving the discrete eigenvalues derived from equation (40) determine electromagnetic and weak susceptibility to the spin 1/2 point particles that themselves possess the non-discrete $\Phi(|m| = 1/2, k)$ with μ^* being μ . For example, the eigenfunction of $\Phi(m = \mp 1/2, m' = -1/2, k)$ is considered to represent the virtual photon state setting up

rotational coordinate of \mathbf{R}^3 -orbital motion of charged ℓ and $\bar{\ell}$, respectively. For the case in which $k \neq 0$, we set to as $k > 0$ without loss of generality, and examined below are the eigenstates of $\Phi(|m| = 1/2, k > 0)$ for $m' = \pm 1/2$ each.

4.2.1. *The case of $m' = 1/2$* Equation (40) for $(m, m') = (1/2, 1/2)$ can be expressed as

$$\tilde{\kappa} + \tilde{k} (1 - 2\tilde{\xi} \cot \tilde{\xi}) = 0. \quad (41)$$

Here, $\tilde{\kappa} = \kappa a$ and $\tilde{k} = ka$ are real, and we have the relation of $\tilde{\kappa} = \pm \sqrt{\tilde{k}^2 + \tilde{\xi}^2}$ in response to equation (36b). Although the root property of equation (40) depends on the sign of $m\kappa$, rather than κ , the case analysis for the sign of κ each is carried out for given m , for an explanation.

The case of $\tilde{\kappa} > 0$ It is natural to consider that the lowest energy kinematics of a “spinning point” reflects a rotational eigenstate accompanied by minimal magnitude of κ . We express $\tilde{\kappa}$ as a function of $\tilde{\xi}$, and write it as $\kappa_{\text{R}}^{(+)} (> 0)$; that is,

$$\kappa_{\text{R}}^{(+)} = \frac{\tilde{\xi} (2\tilde{\xi} \cot \tilde{\xi} - 1)}{\sqrt{(2\tilde{\xi} \cot \tilde{\xi} - 1)^2 - 1}}, \quad \text{for } \tilde{\xi} \cot \tilde{\xi} > 1. \quad (42)$$

Here, the subscript R stands for right-handedness of the helix ($m > 0$) and sign in the superscript indicates the one of $\tilde{\kappa}$. In the domain of definition, i.e., the discrete regions of $\tilde{\xi}$ satisfying $\tilde{\xi} \cot \tilde{\xi} > 1$, investigated is existence of the local minimum of $\kappa_{\text{R}}^{(+)}$. If there exists, we evaluate $\kappa_{\text{R}}^{(+)} = \tilde{\kappa}$, $\tilde{\xi}$, and $\tilde{k} (= \sqrt{\tilde{\kappa}^2 - \tilde{\xi}^2})$ at the stable point: these constitute a set of the eigenvalues for the eigenfunction of Φ . Along this guideline, $\kappa_{\text{R}}^{(+)}$ is plotted in figure 2(a). It is noted that the root space should be restricted to a finite range such that $\tilde{\xi} < \infty$ excluding the set of $\{\infty\}$, which is called later for a specific purpose (section 5.2). Anyhow, one can see that there is no local minimum in the domain. It is thus concluded that for $(m, m', \kappa) = (1/2, 1/2, +)$ exists no eigenstate.

The case of $\tilde{\kappa} < 0$ For equation (41), $-\tilde{\kappa}$ is expressed as a function of $\tilde{\xi}$, to be denoted as $\kappa_{\text{R}}^{(-)} (> 0)$, where the notations are the same as before. This is expressed as

$$\kappa_{\text{R}}^{(-)} = -\kappa_{\text{R}}^{(+)}, \quad \text{for } \cot \tilde{\xi} < 0. \quad (43)$$

In figure 2(b), $\kappa_{\text{R}}^{(-)}$ is plotted; now we find the local minima in the domain wherein $\cot \tilde{\xi} < 0$ is satisfied. Setting $d\kappa_{\text{R}}^{(-)}(\tilde{\xi})/d\tilde{\xi} = 0$ yields the eigenvalue equation for $\tilde{\xi}$, which can be expressed as

$$(\tau - 4v^{-1})(\tau - v^{-1})v^{-1} + \tau = 0, \quad (44)$$

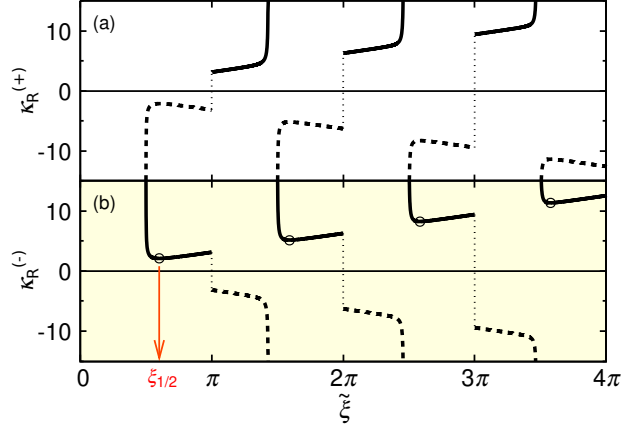


Figure 2. Plots of $\kappa_R^{(+)}(\tilde{\xi})$ [equation (42)] (a) and $\kappa_R^{(-)}(\tilde{\xi})$ [equation (43)] (b). The functions positive in the discrete domains are shown by solid curves. Both figures have a common horizontal axis. In (b), the points at which $\kappa_R^{(-)}$ takes the local minima are indicated by open circles.

Table 1. A set of the discrete eigenvalues $\xi_{m',n}$, $\kappa_{m',n}$, and $k_{m',n}$ for $|m'| = 1/2$ and $n = 1$.

m'	$\xi_{m'}$	$\kappa_{m'}$	$k_{m'}$
1/2	1.891	2.110	0.9363
-1/2	3.445	3.632	1.152

for $v^{-1} < 0$, where $\tau = \tilde{\xi}^{-1}$ and $v = \tan \tilde{\xi}$. The roots of equation (44) are formally numbered such as $n = 1, 2, 3, \dots$ in order from the smaller one, and denoted as $\xi_{1/2,n}$ for $m' = 1/2$. Note that n should be finite, so as to be consistent with the foregoing restriction of root space. It follows that the well-defined $\kappa_{1/2,n} = \kappa_R^{(-)}(\tilde{\xi} = \xi_{1/2,n})$ and $k_{1/2,n} = \sqrt{\kappa_{1/2,n}^2 - \xi_{1/2,n}^2}$ are evaluated, to give $-\kappa_{1/2,n}(\xi_{1/2,n}, k_{1/2,n})$. This means that, even for the previous case in which $\kappa > 0$, we could have the eigenvalues $\kappa_{1/2,n}(\xi_{1/2,n}, k_{1/2,n})$ by the change of $m = 1/2 \rightarrow -1/2$, i.e., $(m, m', \kappa) = (-1/2, 1/2, +)$. In particular, the eigenvalues for $n = 1$ are listed in the upper row of table 1; hereafter, when the root of $n = 1$ is chosen, the subscript indicating it is dropped.

4.2.2. The case of $m' = -1/2$ Equation (40) for $(m, m') = (-1/2, -1/2)$ can be expressed as

$$\tilde{\kappa} - \tilde{k} \left(1 + 2\tilde{\xi} \tan \tilde{\xi}\right) = 0. \quad (45)$$

By the method given above, we look for the eigenvalues equation (45) contains.

The case of $\tilde{\kappa} > 0$ When $\tilde{\kappa}$ of equation (45) as a function of $\tilde{\xi}$ is denoted as $\kappa_L^{(+)}(> 0)$, this can be

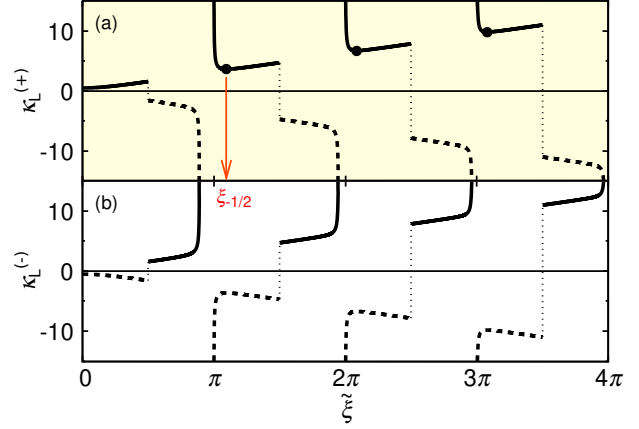


Figure 3. Plots of $\kappa_L^{(+)}(\tilde{\xi})$ [equation (46)] (a) and $\kappa_L^{(-)}(\tilde{\xi})$ (b). The functions positive in the discrete domains are shown by solid curves. Both figures have a common horizontal axis. In (a), the points at which $\kappa_L^{(+)}$ takes the local minima are indicated by filled circles.

expressed as

$$\kappa_L^{(+)} = \frac{\tilde{\xi} \left(2\tilde{\xi} \tan \tilde{\xi} + 1\right)}{\sqrt{\left(2\tilde{\xi} \tan \tilde{\xi} + 1\right)^2 - 1}}, \quad \text{for } \tan \tilde{\xi} > 0, \quad (46)$$

where the subscript L stands for left-handedness of the helix ($m < 0$). If there exists the local minimum of $\kappa_L^{(+)}$ in the domain wherein $\tan \tilde{\xi} > 0$ is satisfied, $\kappa_L^{(+)} = \tilde{\kappa}$, $\tilde{\xi}$, and \tilde{k} are evaluated at the stable point. In figure 3(a), the function $\kappa_L^{(+)}$ is plotted, to show up the profile similar to that seen in figure 2(b), and existence of the local minima in the domain. Setting $d\kappa_L^{(+)}(\tilde{\xi})/d\tilde{\xi} = 0$ yields

$$(\tau + 4v)(\tau + v)v - \tau = 0, \quad (47)$$

for $v > 0$. Equation (47) contains the roots $\tilde{\xi} = \xi_{-1/2,n}$, which determine the values of $\kappa_{-1/2,n} = \kappa_L^{(+)}(\tilde{\xi} = \xi_{-1/2,n})$ and $k_{-1/2,n} = \sqrt{\kappa_{-1/2,n}^2 - \xi_{-1/2,n}^2}$, to give $\kappa_{-1/2,n}(\xi_{-1/2,n}, k_{-1/2,n})$. Especially for $n = 1$, these values are listed in the bottom row of table 1.

The case of $\tilde{\kappa} < 0$ For equation (45), $-\tilde{\kappa}$ is expressed as a function of $\tilde{\xi}$, to be denoted as $\kappa_L^{(-)}(> 0)$. The function $\kappa_L^{(-)} = -\kappa_L^{(+)}$, which is valid for $\tilde{\xi} \tan \tilde{\xi} < -1$, is plotted in figure 3(b). As would be expected, there is no local minimum in the domain: no eigenstate in this case. However, by the change of $m = -1/2 \rightarrow 1/2$, i.e., $(m, m', \kappa) = (1/2, -1/2, -)$, we could have $-\kappa_{-1/2,n}(\xi_{-1/2,n}, k_{-1/2,n})$.

Table 2. Summary of the rotational eigenvalues.

m	m'	$\kappa(> 0)$	$\kappa(< 0)$	Reference ^a
$m'(\text{L})$	$-1/2$	$\kappa_{-1/2}$	—	(35a)
$m'(\text{R})$	$+1/2$	—	$-\kappa_{1/2}$	(35b)
$-m'(\text{R})$	$-1/2$	—	$-\kappa_{-1/2}$	(35c)
$-m'(\text{L})$	$+1/2$	$\kappa_{1/2}$	—	(35d)

^aEquation numbers for the leptonic states that refer to the eigenstates are denoted.

4.3. CP symmetry and chiral asymmetry of helical eigenflows

In light of the allowed combinations of $(m, m', \kappa) = (\pm, \pm, \pm)$, the rotational eigenvalues for $|m| = 1/2$ are summarized in table 2. It is proclaimed that the eigenstates do exist for $m\kappa < 0$, whereas do not for $m\kappa > 0$. For the former, Φ_z of the eigenstates for $(m, m', \kappa) = (-, -, +)$, $(+, +, -)$, $(+, -, -)$, $(-, +, +)$ responds to the term of $J_{-1/2}e^{-i\theta/2}$ in equation (35a), $iJ_{1/2}e^{i\theta/2}$ in (35b), $J_{-1/2}e^{i\theta/2}$ in (35c), and $-iJ_{1/2}e^{-i\theta/2}$ in (35d), respectively, with $\xi = \mu r$ on the common cylindrical base. For the latter, no eigenstate for $(m, m', \kappa) = (-, -, -)$, $(+, +, +)$, $(+, -, +)$, $(-, +, -)$ responds to $J_{-1/2}e^{-i\theta/2}$ in equation (35d), $-iJ_{1/2}e^{i\theta/2}$ in (35c), $J_{-1/2}e^{i\theta/2}$ in (35b), and $iJ_{1/2}e^{-i\theta/2}$ in (35a), respectively, to turn the gauge field coupling off. Transition among lepton doublet: $(\nu_e)_L \rightarrow (e^-)_L$ in β^- -decay can be compared to transition of $\kappa_{1/2} \rightarrow \kappa_{-1/2}$ for $(m, \kappa) = (-, +)$, while $(\bar{\nu}_e)_R \rightarrow (e^+)_R$ in β^+ -decay, to $-\kappa_{1/2} \rightarrow -\kappa_{-1/2}$ for $(m, \kappa) = (+, -)$. The CP transformation can be seen as the flip of $(m, \kappa) = (-, +) \rightleftharpoons (+, -)$ for m' unchanged.

Regarding equation (20), ℓ_L and $(\bar{\ell})_R$ must refer to the eigenfunction of $\Phi(m = -1/2, m' = \mp 1/2, \tilde{\kappa} = \kappa_{\mp 1/2})$ and $\Phi(1/2, \pm 1/2, -\kappa_{\pm 1/2})$, respectively; in particular, charged ℓ and neutral $\bar{\ell}$, to $\Phi(m = m' = -1/2, \kappa_{-1/2})$ and $\Phi(m = m' = 1/2, -\kappa_{1/2})$, respectively. Remarkable is the relation of $\kappa_{-1/2} \neq \kappa_{1/2}$, and chiral asymmetry between L- and R-helix representing the eigenfunctions. This asymmetry is amenable to left-handed selectivity of the charged current weak interaction.

According to these ingredients, we put forth the module representation of

$$\Phi\left(-\frac{1}{2}, -\frac{1}{2}, +\right) \oplus i\Phi^\dagger\left(-\frac{1}{2}, \frac{1}{2}, -\right) =: \Sigma_-, \quad (48a)$$

$$\Phi^\dagger\left(\frac{1}{2}, -\frac{1}{2}, +\right) \oplus i\Phi\left(\frac{1}{2}, \frac{1}{2}, -\right) =: \Sigma_+, \quad (48b)$$

for ℓ_L and $(\bar{\ell})_R$ in equation (19), respectively. Here, Φ^\dagger denotes the non-active counterpart having the inverted m' and κ so that $m\kappa > 0$. The expression of Σ_{\mp} , i.e., the sum of the non-discrete states with

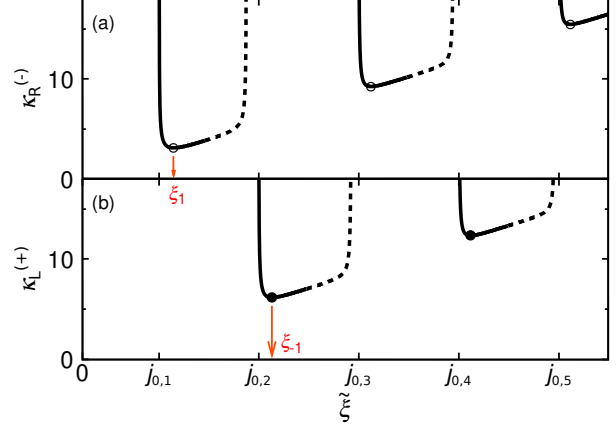


Figure 4. Plots of $\kappa_R^{(-)}(\tilde{\xi})$ [equation (50)] (a) and $\kappa_L^{(+)}(\tilde{\xi}) = -\kappa_R^{(-)}(\tilde{\xi})$ (b). These functions having, respectively, the domain of $j_{0,n'} < \tilde{\xi} < j_{1,n'}$ for odd and even number of n' ($= 1, 2, 3, \dots$) are designated by solid curves. Both figures have a common horizontal axis, on which positions of $j_{0,n'}$ are indicated, in place of scale of the linear axis. The points at which $\kappa_R^{(-)}$ and $\kappa_L^{(+)}$ take the local minima in their domains are indicated by open and filled circles, respectively. The broken curves in (a) and (b) correspond to $\kappa_L^{(-)}$ and $\kappa_R^{(+)}$ for $j_{1,n'} < \tilde{\xi} < j_{2,n'}$ with n' odd and even, respectively (see text).

$\xi = \mu r$ can suitably configure equation (35a) and (35b), respectively.

4.4. Remarks on integer modes

For $m = \pm 1$, we outline the results, in that the eigenstates are related to gauge bosons with the spin $|m|$. One can calculate the discrete eigenvalues basically along the procedure as explained in section 4.2. However, we have only to examine the case of $m = m'$, since $J_{m'}$ and $J_{-m'}$ with m' integer are linearly dependent.

In general, on pattern of existence of the eigenstates, it is found that $\kappa_R^{(-)} (= -\tilde{\kappa} > 0)$ and $\kappa_L^{(+)} (= \tilde{\kappa} > 0)$, respectively, for $(m, \kappa) = (+, -)$ and $(-, +)$, i.e., for $m\kappa < 0$, have locally stable points in their domains. As is, a triad of the well-defined eigenvalues $\xi_{m,n}$, $\kappa_{m,n}$, and $k_{m,n}$ can be obtained. For the mode in which m is an even number, we have $\xi_{m,n} = \xi_{-m,n}$, $\kappa_{m,n} = \kappa_{-m,n}$, and $k_{m,n} = k_{-m,n}$, whereas the odd mode leads to $\xi_{|m|,n} < \xi_{-|m|,n}$, $\kappa_{|m|,n} < \kappa_{-|m|,n}$, and $k_{|m|,n} < k_{-|m|,n}$ (like for $|m| = 1/2$), breaking chiral symmetry. This modal parity stems from the relation of $J_{-m} = (-1)^m J_m$. It is noted that, in the special case in which $m = 0$, spectrum of $\tilde{\kappa}$ is continuous.

For $m = \pm 1$ of particular interest, the eigenvalue equation for $\tilde{\xi}$ is commonly ascribed to

$$J_0^2(\tilde{\xi}) \left[\tilde{\xi} J_0(\tilde{\xi}) - 2J_1(\tilde{\xi}) \right] + J_1^3(\tilde{\xi}) = 0, \quad (49)$$

Table 3. A set of the discrete eigenvalues $\xi_{m,n}$, $\kappa_{m,n}$, and $k_{m,n}$ for $|m| = 1$ and $n = 1$.

$m(=m')$	ξ_m	κ_m	k_m
1	2.857	3.112	1.234
-1	5.937	6.162	1.652

regardless of combination of $(m, \kappa) = (\pm, \pm)$. The $\tilde{\xi}$ -regions allowed are expressed as $j_{0,n'} < \tilde{\xi} < j_{1,n'}$ and $j_{1,n'} < \tilde{\xi} < j_{2,n'}$ for $(m, \kappa) = (\pm, \mp)$ and (\pm, \pm) , respectively, where $j_{m,n'}$ denotes the n' -th zero of $J_m(\tilde{\xi})$. However, one can ascertain that, for the latter, exists no root in equation (49). It should be mentioned that the function of $\tilde{\xi}$ for the case of $(+, -)$, shown in figure 4(a):

$$\kappa_{\text{R}}^{(-)} = -\frac{\tilde{\xi} \left[\tilde{\xi} J_0(\tilde{\xi}) - J_1(\tilde{\xi}) \right]}{\sqrt{\tilde{\xi} J_0(\tilde{\xi}) \left[\tilde{\xi} J_0(\tilde{\xi}) - 2J_1(\tilde{\xi}) \right]}}, \quad (50)$$

is related to the function for the $(-, +)$ case shown in (b), as $-\kappa_{\text{R}}^{(-)} = \kappa_{\text{L}}^{(+)}$. The domains of $\kappa_{\text{R}}^{(-)}$ and $\kappa_{\text{L}}^{(+)}$ are found to be $j_{0,n'} < \tilde{\xi} < j_{1,n'}$ with n' odd and even number, respectively. As seen in figure 4, the values of $\tilde{\xi}$ at which the positive functions of $\kappa_{\text{R}}^{(-)}$ and $\kappa_{\text{L}}^{(+)}$ take the local minima in each domains, namely, the roots of equation (49), denoted as $\xi_{\pm 1, n}$, appear such as $\xi_{1,1}, \xi_{-1,1}, \xi_{1,2}, \xi_{-1,2}, \dots$ in order from the smaller one. It turns out that the eigenvalues of $\xi_{1,n} = \xi_{1,(n'+1)/2}$ for n' odd and $\xi_{-1,n} = \xi_{-1,n'/2}$ for n' even alternately appear. For convenience, the eigenvalues for $n = 1$ are shown in table 3.

5. Observability of the rotational field

5.1. Relation of the field with nonrelativistic kinematics of a fermionic particle

We treat observational issue on the rotational field $\Phi(m = m' = -1/2, \kappa > 0)$: the active module of Σ_- . When regulated by the corresponding eigenfunction, Σ_- should describe a charged, spin 1/2 point particle rotating in an \mathbf{R}^3 -orbit. In the regime in which the regulation is done by the eigenfunction for the common $m = -1/2$, we do not have such a constraint on $k \rightarrow 0$ that has been required for $|m| = 1/2$ system spanning internal pion field to expand as compatible with $|m| = 1$ system. This resembles the situation in which equation (28) is applicable to reproduction of the Cornell potential for $q\bar{q}$ moving nonrelativistically. It is, then, considered that derived from Φ for $k \rightarrow 0$ is kinematics of the charged lepton moving nonrelativistically (i.e., $\beta \rightarrow 0$ and $\bar{\mu} \neq 0$). When $k \rightarrow 0$ is taken for $k \neq 0$ prerequisite to the regulation of Φ , the operation corresponds to

projection of the helical structure onto the cylindrical base. For a spatial transformation involving it, we presume the form of

$$\kappa \mathbf{r} \rightarrow \text{sgn}(\kappa) g_0^{-1} \mu \boldsymbol{\rho}, \quad (51)$$

where $\text{sgn}(\kappa \geq 0) = \pm$, and $\boldsymbol{\rho}$ represents a radial coordinate vector (its initial point = origin “o”) on a complex plane, satisfying $\mu r = \mu |\boldsymbol{\rho}|$.

In view of kinematic states of a spinning point, we see the geometric mechanics that provides fundamental representation of $\text{SU}(2)$, viz., $\mathbf{S} = (\hbar/2)\boldsymbol{\sigma}$, where $\boldsymbol{\sigma}$ stands for the vector of Pauli matrices: $(\sigma_x, \sigma_y, \sigma_z)$ [3]. For this purpose, the charged leptons are represented simply by electron. In the special case of $k = 0$ compared to the rest state, it is trivial that sign of Σ_- is inverted by the rotation of $\theta = 0 \rightarrow 2\pi$, and recovered first by that of 4π . Meanwhile, one could render the rotation center o identical with the \mathbf{R}^3 -coordinate origin O at which the electron is at rest. When making the rotation angle of either $-\theta$ or θ correspond to \mathbf{R}^3 -rotation angle Θ , therefore, Σ_- embodies such a basic property of \mathbf{S} that rotational operator generates $\exp[i\boldsymbol{\Theta} \cdot \mathbf{S}/\hbar]_{|\Theta|=2\pi} = -I$, where $|\boldsymbol{\Theta}| = \Theta$, and $I (= \sigma_x^2 = \sigma_y^2 = \sigma_z^2)$ the unit matrix.

As for $k \neq 0$, we take account of motion of spin and circular orbit of a single electron affected by uniform magnetic field \mathbf{B} , as shown in figure 5(a) (see, e.g. figure 3-3 in [27], and the relevant explanations therein). Concerning access to Φ of the nonrelativistic electron, transformation of $kz \rightarrow g_0^{-1}(1 - \delta_g)\bar{\mu}\zeta$, in conjunction with equation (51), is applied to the phase factor of Φ_z raised to the power of g_0 . Here, μ has been replaced by $(1 - \delta_g)\bar{\mu}$, with δ_g being $1 - \sqrt{1 - \delta} = \delta/2 + \dots$. On the resulting $e^{-i[\theta + (1 - \delta_g)\bar{\mu}\zeta]}$, we impose the lifting shift of $(\theta, \zeta) = (0, 0) \rightarrow (-2\pi, 2\pi\bar{\mu}^{-1})$, which advances the phase. Along with the L/R definition for helix, let negative sign of rotational angles be clockwise. When writing the advancing phase as $\Delta\theta$, to get

$$\delta_g = \Delta\theta/2\pi, \quad (52)$$

this can be compared to the radiative correction term in the g -factor of $2[1 + \Delta\Theta/(2\pi\Gamma)]$, where $\Gamma = (1 - \beta^2)^{-1/2}$, and $\Delta\Theta$, which can be expressed as $\Gamma\Delta\Theta(\Gamma \rightarrow 1)$, is the observed advancing angle of spin precession. For anti-clockwise, $\Theta(= -\theta) = 2\pi$ rotation of unit coordinate vector $\hat{\mathbf{r}}$ as shown in figure 5(b), we find the correspondence between $\Delta\Theta/\Gamma$ and $\Delta\theta$:

$$\Delta\theta \longleftrightarrow \Delta\Theta(\beta \rightarrow 0). \quad (53)$$

5.2. Mechanism advancing spin precession frequency

5.2.1. Coordinate mechanics of the charged fermion
The internal mechanics that determines the value of $\Delta\theta$ must describe the observed kinematics of the electron.

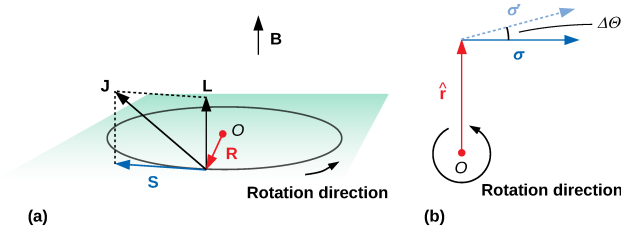


Figure 5. Cyclotron motion of a single electron having the spin \mathbf{S} and its longitudinally polarized state (a), and the corresponding rotation of unit radial vector $\hat{\mathbf{r}} = \mathbf{R}/|\mathbf{R}|$ and change of the polarization for the one orbital turn: $\sigma \rightarrow \sigma'$ (b). In (a), the angular momentum coupling is depicted.

Full information of the kinematic state is contained in the total angular momentum as the coupling of the orbital angular momentum \mathbf{L} and \mathbf{S} :

$$\mathbf{J} = \mathbf{L} + \mathbf{S}, \quad (54a)$$

as shown in figure 5(a). We pay attention to the formalism such that for $\beta \rightarrow 0$, equation (54a) reduces to

$$\mathbf{J} \longrightarrow \mathbf{S}. \quad (54b)$$

Reminding this, we construct for heuristic the rotational internal coordinate that is allied with $\hat{\mathbf{r}}$ and capable of generating σ . By combining the correspondence of $\Phi \leftrightarrow \mathbf{B}$ with equation (5), we prepare replacement of $\Phi \rightarrow i\lambda\mathbf{r}$ (λ constant), allowing for its application to equation (38). Taking this into account, we introduce the covering vector for $\mathbf{J}/\sqrt{3}$, defined by

$$\mathbf{\Lambda} := [\nabla \times \Phi]_{\Phi \rightarrow i\lambda\mathbf{r}} = i\lambda\kappa\mathbf{r}. \quad (55)$$

This reads as follows: the internal quantity $\mathbf{\Lambda}$ is, for $\lambda \rightarrow \hbar$, reflected in the expressions of the orbital angular momentum $-\mathbf{P} \times \mathbf{R}$ and $\mathbf{P} = -i\hbar\nabla$ in \mathbf{R}^3 . To $\mathbf{\Lambda}$ as a primal stuff unifying them, applied is equation (51) for the projective $k \rightarrow 0$. This results in yielding the following form just in parallel with equation (54b):

$$\mathbf{\Lambda} \longrightarrow \mathbf{\Lambda}_0, \quad (56a)$$

where

$$\mathbf{\Lambda}_0 = \text{sgn}(\kappa) i g_0^{-1} \lambda \mu \boldsymbol{\rho}. \quad (56b)$$

In the context, the quantity $\mathbf{\Lambda}_0$ with $\text{sgn}(\kappa) = +$ ought to describe $\mathbf{S}/\sqrt{3}$ of the electron moving nonrelativistically. It is now a matter of normalizing equation (56b), to provide the following symbolic master equation that spin-half particles would refer to:

$$\hat{\sigma} = \text{sgn}(\kappa) i \xi \hat{\rho}, \quad (57a)$$

where

$$\hat{\sigma} = \mathbf{\Lambda}_0 / (\lambda / g_0), \quad \hat{\rho} = \boldsymbol{\rho} / |\boldsymbol{\rho}|, \quad (57b)$$

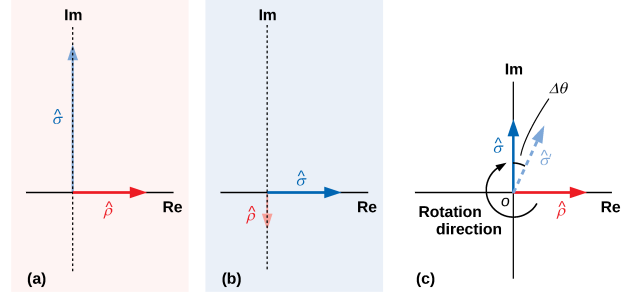


Figure 6. Complex planes indicating, on the real axes, $|\hat{\rho}| = 1$ (a) and $|\hat{\sigma}| = 1$ (b) for a common $\xi (> 1)$, and a normalized complex plane (c) corresponding to figure 5(b).

and $\xi = \mu|\boldsymbol{\rho}|$, which connotes coupling of $\mu|\boldsymbol{\rho}|$ with $\mu^*r =: \xi$ (section 4.1). The detectability owing to $r \rightarrow \infty$ can then be related to setting a stereographic projection point on a sphere so as to cover $\mathbb{C}_{*(-1/2)} \cup \{\infty\}$, where $\mathbb{C}_{*(m')} = \{\mu\boldsymbol{\rho} \in \mathbb{C} \mid 0 < \mu|\boldsymbol{\rho}| \leq \xi_{m'}\}$; its planar shape is the same as that for the Cornell regime. The sphere is incomplete in relation to $\mathbb{C}_{*(m')} \subsetneq \mathbb{C}$. Equation (57a) sustains orthogonality of the base spaces $(\boldsymbol{\rho}, \mathbf{\Lambda}_0)$, serving as the spatio-unifier.

We delve into rotation of $(\boldsymbol{\rho}, \mathbf{\Lambda}_0)$ for $\text{sgn}(\kappa) = +$, in terms of self-consistent procedure of the normalization. First, it is supposed that $\hat{\rho}$ is a basis vector normalized when $\boldsymbol{\rho}$ gets on real axis of the complex plane. Then, trivially $|\hat{\rho}| = 1$ is established on the real axis, and the real basis vector is to come out in $\hat{\mathbf{r}}$. The vector configuration of equation (57a) on this plane is illustrated in figure 6(a), providing a value of ξ larger than unity. Second, supposed is that $\hat{\sigma}$ is another independent basis vector normalized when $\boldsymbol{\rho}$ rotates by $-\pi/2$ to be purely imaginary and $\mathbf{\Lambda}_0$ gets on the real axis. Recalling $\lambda \rightarrow \hbar$, we identify $|\mathbf{\Lambda}_0| = \lambda/g_0$ with the detectable $|\mathbf{S}|/\sqrt{3} = \hbar\sqrt{s(s+1)}/\sqrt{3} = \hbar/2$ for $s = 1/2$. Then, $|\hat{\sigma}| = 1$ is established on the real axis; the vector configuration of equation (57a) on the second plane is shown in figure 6(b).

Besides, the vector configuration of $(\hat{\mathbf{r}}, \sigma)$ [figure 5(b)] is recast to the configuration of $(\hat{\rho}, \hat{\sigma})$ on a normalized complex plane, which is shown in figure 6(c). This can be regarded as superposition of $\hat{\rho}$ on the first plane (a) and $\hat{\sigma}$ put on the imaginary axis by the rotation of $\pi/2$ on the second plane (b). For Θ and θ as rotation angles of $\hat{\mathbf{r}}$ and $\hat{\rho}$, respectively, we have $\Theta = -\theta$, and therefore, $\hat{\rho}$ rotated by -2π is to coincide with the initial one. On the other hand, $\sigma \rightarrow \sigma'$ incidental to the one turn of $\hat{\mathbf{r}}$ should be described by $\hat{\sigma} \rightarrow \hat{\sigma}'$ with $\Delta\theta$, where invariant of the magnitude: $|\hat{\sigma}| = |\hat{\sigma}'| = 1$ is imposed. Then, $\hat{\sigma}$ is responsible for $\sigma/\sqrt{3}$, on account of $\hat{\sigma}^2 \rightarrow \sigma^2/3 = I$. It turns out that $\mathbf{\Lambda}_0 = (\lambda/g_0)\hat{\sigma}$ is, for $\lambda\hat{\sigma} \rightarrow \hbar\sigma/\sqrt{3}$, reflected in $\mathbf{S}/\sqrt{3}$.

5.2.2. *Concept of coordinate self-renormalization* It can be claimed that $\hat{\rho}$ represents $(n_d - 1)$ -dimensional projective plane of \mathbf{r}^{n_d} space having the dimensions of $n_d = 3$, and $\hat{\sigma}$ does likewise. In addition, ξ takes on one degree of freedom that mediates between those two spaces. Although $\hat{\rho}$ and $\hat{\sigma}$ are distinguished from one another, $\hat{\sigma}$ in figure 6(b) embodies $\hat{\rho}$ in (a) on the real axis, so that observer has no way to distinguish both the basis vectors for the comparison. This suggests such an isotopic relation of $\hat{\sigma}$ to $\hat{\rho}$ that after the aforementioned clockwise quarter-turn of $\boldsymbol{\rho}$, $\hat{\sigma}$ maintains gauge of the real axis that connects to \mathbf{R}^3 , on behalf of $\hat{\rho}$ that was there before the turn. This instant, $\hat{\rho}$ is on the imaginary axis, having the magnitude of $1/\xi$. That is, as seen in figure 6(a,b), the turn leads to the shrinkage of $\hat{\rho}$, which is undetectable at this moment. Especially for the one clockwise turn, the vector shrunk up gets again on the real axis, to be expressed as $\Delta\hat{\rho} = (1/\xi^4)\hat{\rho}$. This must be an observable portion. Meanwhile, for the one turn of $\hat{\rho}$ in figure 6(c), postulated is invariant of $|\hat{\rho}|$. To reconcile the both, we should consider that the appearance of $\hat{\rho}$ having $|\hat{\rho}| = 1$ results from superposition of $\Delta\hat{\rho}$ on a coordinative vector tentatively normalized on the real axis in another way. Expected is that the scalar ξ plays a key rôle in the radical process, referred to as coordinate self-renormalization (CSR), hereafter.

Concerning the pre-normalization, it is reasonable to recall the critical value of ξ , i.e., $\tilde{\xi} = \mu^* a$, and introduce $\hat{\rho}_a = \boldsymbol{\rho}/a$ having its magnitude of $\xi/\tilde{\xi}$. By employing them, one can rewrite $\xi\hat{\rho}$ as $\tilde{\xi}\hat{\rho}_a$ in equation (57a). This signifies the coordinate setup that enables Φ to refer to the corresponding eigenfunction. Noted is $|\hat{\rho}_a| < |\hat{\rho}|$ because of $\xi < \tilde{\xi}$. Taking these into account, we make the following transformation that undertakes CSR:

$$\hat{\rho}_a \longrightarrow \hat{\rho} = \hat{\rho}_a + \Delta\hat{\rho}, \quad \text{on } \Re. \quad (58)$$

For $\Delta\hat{\rho}$ to be observable would require complementation between $\Delta\hat{\rho}$ and $\Delta\theta$ related to the displacement of $\hat{\sigma}$, in harmony with the isotopic relation between $\hat{\rho}$ and $\hat{\sigma}$. That is, it is supposed that the transformation of

$$\hat{\sigma} \longrightarrow \hat{\sigma}' = \hat{\sigma} + \Delta\hat{\sigma}, \quad (59)$$

is self-consistently carried out such that the following relation is satisfied:

$$\Delta\hat{\rho} = \Re(\Delta\hat{\sigma}), \quad (60)$$

as displayed in figure 7.

5.3. Generation of numerical value compared to α

From equation (60), we have $|\Delta\hat{\rho}| = |\hat{\sigma}'| \sin \Delta\theta$. Equating this to the relation of $|\Delta\hat{\rho}| = 1/\xi^4$ yields the equation that connects ξ and $\Delta\theta$:

$$\xi^{-4} = \sin \Delta\theta. \quad (61)$$

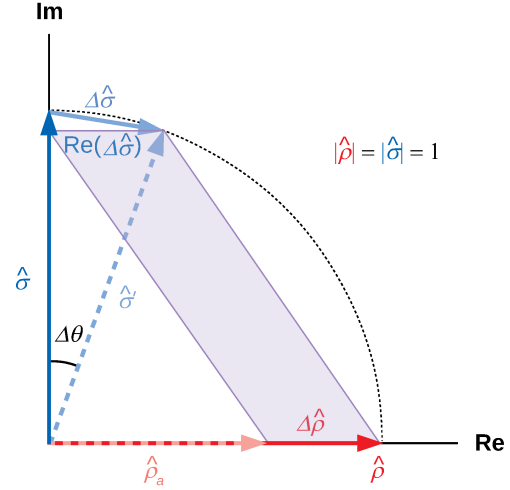


Figure 7. A schematic to explain how to harmonize the transformation of $\hat{\rho}_a \rightarrow \hat{\rho}$ with $\hat{\sigma} \rightarrow \hat{\sigma}'$. The dotted curve corresponds to equator of the Riemann sphere.

Another equation can be derived from $\xi|\hat{\rho}| = \tilde{\xi}|\hat{\rho}_a|$. Noted here is that the vector equation (58) operates on the real axis, thereby giving the relation of the magnitude, $|\hat{\rho}_a| = 1 - |\Delta\hat{\rho}|$. Hence, we have

$$\xi = \xi_{-1/2} (1 - \xi^{-4}), \quad (62)$$

where $\tilde{\xi}$ has been set to the critical value in $\mathbb{C}_{*(-1/2)}$, which provides the minimum radius of cylinder to confine $\Phi(m = m' = -1/2, \kappa > 0)$. This gauge-fixing enables the corresponding eigenfunction to regulate the Φ , properly connecting $\boldsymbol{\rho}$ with \mathbf{R} . Physically, this completes the radical coupling of the rotating electron with virtual photon. Equations (61) and (62) give a set of solutions of ξ and $\Delta\theta$.

In order to highlight the physical correspondence, we approximately solve them, assuming $\Delta\theta \ll 1$. When ignoring $\sim (\Delta\theta)^3$ and the higher order terms, equation (61) reduces to

$$\xi^{-4} \cong \Delta\theta. \quad (63)$$

Meanwhile, it is found that within the common approximation, equation (62) allows the expression of $\xi^{-4} \cong \xi_{-1/2}^{-4} / (1 - 4\xi_{-1/2}^{-4})$.

Thus, if only the numerical value of $\xi_{-1/2}$ is given (cf. table 1), one can algebraically calculate the values of ξ and $\Delta\theta$ from equations (63) and (64). Making use of equation (63), equation (53) is cast to

$$\sim \xi^{-4} \longleftrightarrow \Delta\theta(\beta \rightarrow 0). \quad (65)$$

This means that, at least, the scalar quantity ξ^{-4} shall indicate a value comparable to α [41]. Substituting $\xi_{-1/2}^4 \cong 141$ into equation (64) results certainly in yielding

$$\xi^4 \cong 137, \quad (66)$$

so that the assumption of $\Delta\theta \ll 1$ is justified. It is remarked that the result remains unchanged for the antiparticle, because the CSR operates in chiral relation, i.e., inverse rotation ($m = -m' > 0$) of the spatio-unifier with $\text{sgn}(\kappa) = -$, and it is regulated commonly by $\mathbb{C}_{*(-1/2)}$.

The regulated CSR brings about clock in effect, as a tick of $\Delta\theta = 2\pi\delta_g$ measures out one cyclotron-period (frequency of light) independently of electron velocity. Accordingly, the scalar correction in g can be regarded as modest appearance of one-dimension of time as the degree of freedom of ξ , which is released through the dynamical mechanism that properly connects two \mathbf{r}^{n_d} spaces (a complex n_d -dimensional space) with \mathbf{R}^{n_d} space. This means that conceivable dimensions of space-time are $3n_d + 1 = 10$, and total degrees of freedom amount to 11; this number appears to coincide with that as a far-reaching consequence in [42]. Logical necessity of the extra-dimensions, and equation (66) as well, imply that a principle of unification of forces may be self-contained within the present framework [32, 43, 44], though the detail on gravitational force is somewhat beyond the scope of this paper.

The scale of $\sim \xi^{-4}$ can be interpreted as origin of electric energy accompanying point charge excited in vacuum. Then, inequality of $\xi^{-4} > \xi_{-1/2}^{-4}$ is amenable to the well-established QED vacuum picture in which net charge decreases outward due to electrostatic shielding effect by the polarization of virtual electron-positron pairs. Thickness of the imperfect shielding shell reflects $\Delta\xi = \xi_{-1/2} - \xi$. Letting the observed elementary charge and theoretical charge be denoted as e and e_{th} , respectively, we have

$$e^2 = e_{\text{th}}^2 / (1 - \varrho), \quad (67)$$

with ϱ constant, in natural units (e.g. [14]). Its correspondence to equation (64) is pronounced. We find that the finite ϱ , by which a logarithmically diverging term has been replaced, reflects the quantity of $\sim 4\xi_{-1/2}^{-4}$, to be expressed as $4e_{\text{th}}^2$ in a good approximation. Physical meaning of electric charge renormalization can be attributed to the chiral symmetric CSR regulated by a rotational eigenvalue for $m' < 0$.

6. The compatibility with the standard model

We survey how the current theory could be linked to the standard model that systematically describes almost all experimental results with highest accuracy. The arguments expanded below are *not* intended as a trial of updating the completed main body of literature, but concise notification of the relevant geometrical corollary, which may provide clues to go beyond the rigorous framework.

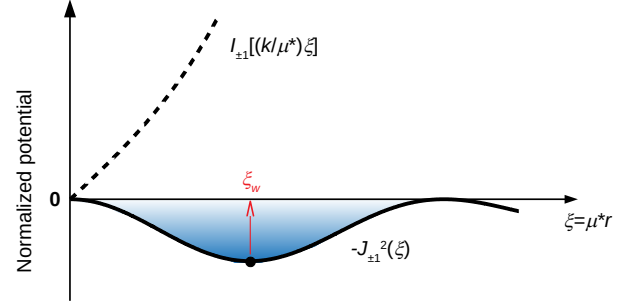


Figure 8. The transformation of the cylindrical functions, $I_{\pm 1} \rightarrow -J_{\pm 1}^2$, caused by equation (68). On the horizontal axis, ξ_w denotes the value of ξ at which the resulting function as the normalized potential $U_{\pm}(\xi)/\phi_{\pm 1}^2$ (solid curve) gives a minimum value.

6.1. Quark fractional charge

Cope with the generation mechanism of quark electric charge, which must be connected with the CSR generating α . This is a subject to the electroweak interaction in the closed \mathbf{R}^{*3} -space. Return to equation (23) with $|m| = 1$, and reconsider the region of $r \rightarrow \infty$ so that the solution can be expressed as $\eta(kr) \sim I_{\pm 1}(kr) \gg K_{\pm 1}(kr)$ (section 4.1). This means that, by largely separating $q\bar{q}$ pair without violating color superconductivity phase, we highlight potential energy of strong force, though in reality the separation ends up with newly creating meson. The internal k -transformation applied to $I_{\pm 1}(kr)$ is recast to the form of

$$kr \rightarrow \varphi := -i\xi, \quad (68)$$

with $\xi := \mu^*r$. It is considered that, the process in which $W^{\pm,0}$ and B^0 particles appear is signified by the transformation of $\eta(kr)$ owing to equation (68). Transformation of internal harmonic potential, parallel to equation (33), is written as follows:

$$\eta^{g_0}(kr) \rightarrow U_{\pm}(\xi) = -\phi_{\pm 1}^2 J_{\pm 1}^2(\xi). \quad (69)$$

Equation (69) could represent generation of the internal potential that works for $\ell\bar{\ell}$ pair separated, in dual relation to equation (33) that represents generation of the external potential of $q\bar{q}$ pair confined. For convenience, the function transformation $I_{\pm 1}(kr) = I_{\pm 1}[(k/\mu^*)\xi] \rightarrow -J_{\pm 1}^2(\xi)$ is shown in figure 8. Since $\phi_{\pm 1}J_{\pm 1}(\xi)$ could constitute Φ_z , it is reasonable to suppose, as virtual photon of charged ℓ is represented by $\Phi(m = m' = -1/2, \kappa_{-1/2})$, that the generated gauge fields are represented by $\Phi(m = m' = \pm 1, \mp \kappa_{\pm 1})$. Henceforth, we refer to such $m = m'$ eigenflows as Φ_m .

We focus on the second equation of (19), which can be decomposed into $d_{(-1/2)} \rightarrow u_{(1/2)} + W_{(-1)}^-$ and $W_{(-1)}^- + \nu_{e(1/2)} \rightarrow e_{(-1/2)}^-$. Here, the values in

the brackets indicate the third component of the weak isospin, T_z . Extending the correspondence between $e_{(-1/2)}^-$ and $\Phi_{-1/2}$, we make the one between T_z and m (in Φ_m) for particle species endowed with negative T_z and negative charge. The Yukawa interaction is rewritten as

$$[d_L + (\bar{u})_R] \longrightarrow W^-, \quad W^- \longrightarrow e_L^- + (\bar{\nu}_e)_R. \quad (70)$$

The square bracket emphasizes the fact that the $d\bar{u}$ pair is confined in the closed space of pion interior.

In that regard, we read that the left-handed d_L , which acts commonly with e_L^- on the charged current interaction, refers to CSR subject to the master equation (57a), as basic internal mechanics of $T_z = -1/2$ [$1/2$ for e_R^+ and $(\bar{d})_R$]. Respecting the rotational motion of e_L^- , the CSR to which the base gauge of $\Phi_{-1/2}$ contributes is found to set up a proper rotational coordinate in the \mathbf{R}^3 space that allows for the orbit. This setup is none other than development of electromagnetic potential. On the basis of this idea, we reconsider the charged current interaction of d_L (undergoing rotational motion in the closed space) with W^- . Expected is that the CSR to which the base gauge of Φ_{-1} contributes is called for setting up a proper coordinate, i.e., developing the interaction potential, in the closed space of $J^P = 0^-$ particle. In particular, the CSR that refers to $\mathbb{C}_{*(-1)}$ must determine the charge of d_L , in the same way of the determination of e for which $\mathbb{C}_{*(-1/2)}$ is referred. In this regime, the projective $k \rightarrow 0$ as a premise of equation (57a) signifies the lowest energy excitation of the pion, rather than kinematic state of the constituent quarks.

From this notion follows: the ξ^{-4} scale of equation (64) of which $\xi_{-1/2}$ is replaced by ξ_{-1} must be responsible for square of the d quark charge e_q . This replacement owes to base coupling between $\Phi_{-1/2}$ and Φ_{-1} via ξ . As a consequence, we have the following expression compared to $\sqrt{e_q^2/e^2} = 1/3$:

$$\sqrt{(\xi_{-1/2}^4 - 4)/(\xi_{-1}^4 - 4)} \cong 0.333, \quad (71)$$

with $\xi_{-1}^4 \cong 1240$ (cf. table 3).

6.2. Symmetry breaking and mass generation

We further examine equation (69), in terms of the mass change $m_W \rightarrow m_{\ell, \bar{\ell}}$ in the second equation of (70). By the transformation, the value of ξ at which the potential indicates the minimum changes from 0 to the well-defined $\xi_w (\neq 0)$. This feature can be seen in figure 8. The value of ξ_w characterizes the quantity μ^* involved in Φ_{-1} , so that ξ_w must be reflected in m_W .

For real ξ , expansion of $J_{\pm 1}^2(\xi)$ can be expressed as a function of $\xi^2 = \varphi^* \varphi$, where the asterisk signifies

the complex conjugate. Accordingly, we have

$$U_{\pm}(\varphi^* \varphi) = -\frac{\phi_{\pm 1}^2}{4} \left[\varphi^* \varphi - \frac{1}{4} (\varphi^* \varphi)^2 + \mathcal{O}((\varphi^* \varphi)^3) \right]. \quad (72)$$

For a comparison, invoked is the standard vacuum model [23], in which one assumes condensate of complex scalar field ψ . For the ψ themselves the interaction potential is written in the approximate form of

$$U(\psi^* \psi) \cong \mu_m^2 \psi^* \psi + \varsigma (\psi^* \psi)^2, \quad (73)$$

where μ_m and ς constants. The vacuum state can be represented by the expectation of ψ , such as $\langle \psi \rangle_0 = 0$ for $\mu_m^2 > 0$: the value of $\sqrt{\psi^* \psi}$ at which U indicates the minimum. As for $\mu_m^2 < 0$, it is found that U indicates the minimum at $\psi^* \psi = -\mu_m^2/2\varsigma$, so that

$$\langle \psi \rangle_0 = \sqrt{-\mu_m^2/2\varsigma}, \quad (74)$$

which linearly couples with m_W . The excitation from $\langle \psi \rangle_0$ can be expressed by $\psi = \langle \psi \rangle_0 + H/\sqrt{2}$, where H the Higgs field. It appears that $U_{\pm}(\varphi^* \varphi)$ of equation (72) serves as an analytic function representation for $U(\psi^* \psi)$ with $\mu_m^2 < 0$. Approving the correspondence $\varphi^* \varphi \leftrightarrow \psi^* \psi$ results in

$$\sqrt{\varphi^* \varphi} = \xi_w \longleftrightarrow \langle \psi \rangle_0, \quad (75)$$

which supports the relation of $\xi_w \propto m_W$. The key equation (68) that brings about ξ_w can be regarded as a trigger of the spontaneous symmetry breaking.

In terms of the connection with the chiral asymmetry of $\Phi_{\pm|m|}$, recall that Σ_+ of $(\bar{\nu}_e)_R$ refers to $\Phi_{1/2}$. It is reasonable to suppose, from this, that the spin 1 neutral boson that can interact with right-handed particles, namely, B^0 , reflects Φ_1 . For the eigenvalue, reminding that ξ_{-1} contributes to determine e_q of the $J^P = 0^-$ particle, we conjecture that its counterpart, ξ_1 , indicates mass of 0^+ particle, specifically, the Higgs boson mass m_H . The point is that, provided a pair of $\Phi_{\pm 1}$ shares the same base coordinate, ratio of ξ_1/ξ_w is to indicate mass ratio of m_H/m_W . The specified values of $\xi_1 \cong 2.86$ and $\xi_w \cong 1.84$ give $\xi_1/\xi_w \cong 1.55$. Indeed, this accords with $m_H/m_W \cong 1.55$ for the experimental values of $m_W \cong 80.4 \text{ GeV}/c^2$ [45] and $m_H \cong 125 \text{ GeV}/c^2$ [46].

Since $\xi_w = \sqrt{\varphi^* \varphi} \leftarrow \xi_1$ is responsible for $m_W \leftarrow m_H$, the concerned $m_W \rightarrow m_{\ell, \bar{\ell}}$ should reflect $\xi_w \rightarrow \xi_{\mp 1/2}$, which cooperates with system transformation of $|m| = 1 \rightarrow 1/2$. The base coupling $\sqrt{\varphi^* \varphi} = \xi_{\mp 1/2}$ is necessary for the regulated rotation of Φ (in Σ_{\mp}), to operate on $U_{\mp}(\varphi^* \varphi)$. In the context, $\xi_1 \rightarrow \xi_{\mp 1/2}$ symbolically represents a process in which inertial mass of $m_{\ell, \bar{\ell}}$ is imprinted in vacuum. When comparing $\xi = \xi_{-1/2} - \Delta\xi \rightarrow \xi_{-1/2}$ to mass renormalization of a charged lepton, $\xi \rightleftharpoons \xi_{-1/2}$ signifies complementation between the mass and charge renormalization.

We attempt to relate the imprint of m_ℓ and $m_{\bar{\ell}}$ to excitation of the φ -field in U_{\mp} . The excitation energies denoted as $\omega_{-1/2}$ and $\omega_{1/2}$ are given by

$$\omega_{-1/2} = U_-(\xi_{-1/2}) - U_-(\xi_w), \quad (76a)$$

$$\omega_{1/2} = U_+(\xi_{1/2}) - U_+(\xi_w). \quad (76b)$$

Noticed is that if $\phi_1^2/\phi_{-1}^2 \sim \mathcal{O}(1)$, we have $\omega_{1/2} \ll \omega_{-1/2}$, because of $U_+(\xi_w) \approx U_+(\xi_{1/2})$ stemming from $\xi_w \sim \xi_{1/2}$. Equations (76a) and (76b) can be compared to the internal mass of Σ_{\mp} analogous to m_π . From this view, invoked is the Gell-Mann-Oakes-Renner relation indicating that m_π^2 should be proportional to mass of quarks constituting the meson [47]. In this analog, we read ratio of $m_{\bar{\ell}}/m_\ell$ as reflecting $(\omega_{1/2}/\omega_{-1/2})^2 \cong 3.53 \times 10^{-6}(\phi_1^2/\phi_{-1}^2)^2$, which is estimated below.

6.3. A hypothetical, radical representation of the electroweak coupling

Extending the indication of $\phi_{-1/2}^2 \rightarrow e^2$ (section 4.1), we expect $\phi_{-1}^2 \rightarrow g^2$ and $\phi_1^2 \rightarrow g'^2$, where g (resp. g') denotes strength of coupling of W (resp. B^0) boson with the weak isospin (resp. weak hypercharge) of the left-handed (resp. both-handed) particles. This implies that mode coupling among Φ_m , with ϕ_m being the strength, describes the electroweak coupling. In this aspect, we revisit the orthogonal decomposition of κ_m -spectrum: (ξ_m, k_m) . As we have seen, the ξ -space is used for coupling with matter fields, such that $m_H \rightarrow m_{\ell, \bar{\ell}}$ goes for ξ_m with $m = 1 \rightarrow \mp 1/2$. Herewith, considered is that the \tilde{k} -space is used for the concerned mode coupling, thereby representing gauge field unification. Synchronizing with the mass pointer, $(g, g') \rightarrow e$ as the charge pointer is to go for k_m with $m = \mp 1 \rightarrow -1/2$.

A vital clue to the relation between ϕ_m and k_m can be found in equation (25), that is, the coupling of cylindrical functions of order $m = \pm 1$ utilizing the common k . An attention should be paid to the ratio of $c_{-1}^2/c_1^2 \sim \tilde{k}^4$ self-contained in equation (25), which plays a crucial rôle in quark confinement. Notice that confinement of leptonic fields inside the cylinder of $\Phi_{-1/2}$, which is compared to perfectly conducting wall, resembles the quark confinement. Hence, as compatible with the k -scaling form, we describe the multi-mode coupling among Φ_m . At this juncture, we introduce hyper coupling constant defined by $\phi_P^2 = (\xi_{-1/2} k_{-1/2})^{-4}$, and suppose that modules of Φ_m are self-adjusted such that their intensities satisfy $\phi_m^2/\phi_P^2 = k_m^4$ each. Then, we have the chain rule for $m = -1/2, -1$, and 1 , expressed as follows:

$$\phi_P^2 = \frac{\phi_{-1/2}^2}{k_{-1/2}^4} = \frac{\phi_{-1}^2}{k_{-1}^4} = \frac{\phi_1^2}{k_1^4}. \quad (77)$$

Specifically, we obtain the key ratio evaluated as

$$\phi_{-1/2}^2/\phi_{-1}^2 = (k_{-1/2}/k_{-1})^4 \cong 0.236. \quad (78)$$

This should be compared with $e^2/g^2 = \sin^2 \theta_W$ in a low energy region, where θ_W the Weinberg angle, and agrees with the experimental data [around 0.236 (marginally smaller than the standard model output of about 0.239) from atomic parity violation in sub- 10^{-2} GeV range; see, e.g. figure 10.2 in [45], and references therein]. Also, $\phi_1/\phi_{-1/2} = (k_1/k_{-1/2})^2 \cong 1.14$ is compared with g'/e , to be almost consistent with the corresponding ratio of m_Z/m_W , where m_Z the Z boson mass.

Moreover, the theoretical value of $m_{\bar{\nu}_e}/m_\ell$ works out, by letting $\phi_1^2/\phi_{-1}^2 = (k_1/k_{-1})^4$ in the foregoing expression of $(\omega_{1/2}/\omega_{-1/2})^2$, at 3.41×10^{-7} . Making this correspond to mass ratio of $\bar{\nu}_e$ to e^- , the $\bar{\nu}_e$ mass is estimated

$$m_{\bar{\nu}_e} \cong 174 \text{ meV}/c^2, \quad (79)$$

as consistent with the experimental upper limit on electron-based $\bar{\nu}$ mass [48]. The direct neutrino mass experiment that covers energy range of equation (79) [49] is awaited to verify the proposed scenario.

7. Conclusions

In conclusion, we have explored geometrical structure of particles having no extractable substructure. Analogy of spatial change of massive photon state has been made to spatial transformation indicative of elementary excitation of particles. Entity of cylindrical space spanning harmonic function has been revealed in an infinitesimal region with extra-dimensions. It has been demonstrated that the Cornell and Yukawa potential are reproducible by applying the spatial transformation to the internal harmonic function. In the cylindrical space, we have introduced the rotational field as a module capable of describing matter and gauge particles. The field, which satisfies rotational eigenvalue equation, resides in the extra-dimensional space; it is updated, genuine recurrence of the Chandrasekhar-Kendall solution for Gromeka-Beltrami flow. The rotational eigenstates reflected in electromagnetic susceptibility have been investigated in details. A module representation of spin-half Lie algebra has been proposed which could reproduce the wavefunction and Coulomb potential for electron.

From the rotational eigenvalue equation, we have drawn a spatio-unifier, which establishes isotopic relation between internal coordinate space and angular momentum space. Rotating the unifier, we obtained a mechanical sequence to maintain those basis vectors, as responsible for cyclotron motion of a single electron with its spin precession. It has been suggested that the coordinate self-renormalization regulated by a specified rotational eigenvalue could be compared to QED renormalization. We found that the radical process completing spatiotemporal setup yields a numerical

value comparable to the electromagnetic coupling constant in the nonrelativistic limit.

Chiral asymmetry of rotational eigenfunctions has been connected with parity violation in electroweak interaction. A likely consequence is that the left-handed eigenflows $\Phi_{-1/2, -1}$ are involved in determining negative charge of (regular) lepton and quark. Multi-mode coupling of $\Phi_{-1/2, \mp 1}$ could radically represent the electroweak coupling, generating a numerical value comparable to the Weinberg angle measured at low energy. While the theory is hypothetical as a whole, noticeable is that the original scenario concerning lepton mass imprint will be testable by forthcoming neutrino mass experiments.

The rotational field is of the helical geometry that enables us to describe a classically indescribable two-valuedness (“klassisch nicht beschreibbare Art von Zweideutigkeit” [50, 51]) by the single-valued functions. The theory supports a common image of cosmic helices not only for the structure of fermionic particles, but for a unified structure including gauge bosons. This means that it seems as if collective dynamics of plasma evolving toward an energy relaxed state refers to the internal structure of particles constituting the macroscopic plasma. I hope the present ideas shed light on a variety of fields.

References

- [1] Dehmelt H 1988 A Single Atomic Particle Forever Floating at Rest in Free Space: New Value for Electron Radius *Phys. Scr.* **T22** 102
- [2] ATLAS Collaboration Aad G *et al* 2020 Search for Magnetic Monopoles and Stable High-Electric-Charge Objects in 13 TeV Proton-Proton Collisions with the ATLAS Detector *Phys. Rev. Lett.* **124** 031802
- [3] Pauli W Jr 1927 Zur Quantenmechanik des Magnetischen Elektrons *Zeit. f. Phys.* **43** 601
- [4] Friedrich J and Walcher Th 2003 A Coherent Interpretation of the Form Factors of the Nucleon in Terms of a Pion Cloud and Constituent Quarks *Euro. Phys. J. A* **17** 607
- [5] Alfvén H 1981 *Cosmic Plasma* (Dordrecht: Reidel)
- [6] Durrer R and Neronov A 2013 Cosmological Magnetic Fields: Their Generation, Evolution and Observation *Astron. Astrophys. Rev.* **21** 62
- [7] Broderick A E and Loeb A 2009 Signatures of Relativistic Helical Motion in the Rotation Measures of Active Galactic Nucleus Jets *Astrophys. J.* **703** L104
- [8] Woltjer L 1958 A Theorem on Force-Free Magnetic Fields *Proc. Nat. Acad. Sci.* **44** 489
- [9] Taylor J B 1986 Relaxation and Magnetic Reconnection in Plasmas *Rev. Mod. Phys.* **58** 741
- [10] Burlaga L F 1988 Magnetic Clouds and Force-Free Fields with Constant Alpha *J. Geophys. Res.* **93** 7217
- [11] Plunkett S P, Vourlidis A, Šimberová S, Karlický M, Kotrč P, Heinzel P, Kupryakov Yu A, Guo W P and Wu S T 2000 Simultaneous SOHO and Ground-Based Observations of a Large Eruptive Prominence and Coronal Mass Ejection *Solar Phys.* **194** 371
- [12] The Event Horizon Telescope Collaboration Akiyama K *et al* 2019 First M87 Event Horizon Telescope Results. I. The Shadow of the Supermassive Black Hole *Astrophys. J.* **875** L1
- [13] Ford H C, Harms R J, Tsvetanov Z I, Hartig G F, Dressel L L, Kriss G A, Bohlin R C, Davidsen A F, Margon B and Kochhar A K 1994 Narrowband HST Images of M87: Evidence for a Disk of Ionized Gas around a Massive Black Hole *Astrophys. J.* **435** L27
- [14] Feynman R P 1961 *The Theory of Fundamental Processes* (Reading: Addison-Wesley) Chap 29
- [15] Sommerfeld A 1916 Zur Quantentheorie der Spektrallinien *Ann. d. Phys.* **51** 1
- [16] Beltrami E 1889 Considerations on Hydrodynamics *Rendiconti del Reale Istituto Lombardo, Series II* vol 22 trans G Filippini 1985 *Int. J. Fusion Energy* **3**(3) 53
- [17] Lee T D and Yang C N 1956 Question of Parity Conservation in Weak Interactions *Phys. Rev.* **104** 254
- [18] Wu C S, Ambler E, Hayward R W, Hoppes D D and Hudson R P 1957 Experimental Test of Parity Conservation in Beta Decay *Phys. Rev. Lett.* **105** 1413
- [19] Bostick W H 1985 The Morphology of the Electron *Int. J. Fusion Energy* **3**(1) 9
- [20] Eichten E, Gottfried K, Kinoshita T, Lane K D and Yan T -M 1978 Charmonium: The model *Phys. Rev. D* **17** 3090
Eichten E, Gottfried K, Kinoshita T, Lane K D and Yan T -M 1980 *Phys. Rev. D* **21** 313 (Erratum)
- [21] Yukawa H 1935 On the Interaction of Elementary Particles. I *Proc. Phys. Math. Soc. Japan* **17** 48
- [22] Gell-Mann M 1964 A Schematic Model of Baryons and Mesons *Phys. Lett.* **8** 214
- [23] Higgs P W 1964 Broken Symmetries and the Masses of Gauge Bosons *Phys. Rev. Lett.* **13** 508
- [24] Glashow S L 1961 Partial-Symmetries of Weak Interactions *Nucl. Phys.* **22** 579
- [25] Weinberg S 1967 A Model of Leptons *Phys. Rev. Lett.* **19** 1264
- [26] Salam A 1968 Weak and Electromagnetic Interactions *Elementary Particle Theory* ed N Svartholm (Stockholm: Almqvist & Wiksell) p 367
- [27] Sakurai J J 1967 *Advanced Quantum Mechanics* (Reading: Addison-Wesley)
- [28] Sir Thomson J J 1927 The Electrodeless Discharge through Gases *Proc. Phys. Soc.* **40** 79
- [29] Tonks L and Langmuir I 1929 Oscillations in Ionized Gases *Phys. Rev.* **33** 195
- [30] Einstein A 1905 Zur Elektrodynamik bewegter Körper *Ann. d. Phys.* **17** 891
- [31] Einstein A 1916 Die Grundlage der allgemeinen Relativitätstheorie *Ann. d. Phys.* **49** 769
- [32] Heisenberg W 1958 *Wandlungen in den Grundlagen der Naturwissenschaft* (Stuttgart: S. Hirzel Verlag)
- [33] Schwarzschild K 1916 Über das Gravitationsfeld eines Massenpunktes nach der Einsteinschen Theorie *Sitzungsber. Preuss. Akad. Wiss. Berlin* (Math. Phys.) **7** 189
- [34] Watson G N 1958 *A treatise on the Theory of Bessel Functions* (London: Cambridge Univ. Press)
- [35] Joukowski N 1910 Über die Konturen der Tragflächen der Drachenflieger *Zeit. f. Flugtech. Motorluft.* **1** 281
- [36] Wilson K G 1974 Confinement of Quarks *Phys. Rev. D* **10** 2445
- [37] Hasegawa A and Mima K 1977 Stationary Spectrum of Strong Turbulence in Magnetized Nonuniform Plasma *Phys. Rev. Lett.* **39** 205
- [38] Honda M, Meyer-ter-Vehn J and Pukhov A 2000 Collective Stopping and Ion Heating in Relativistic-Electron-Beam Transport for Fast Ignition *Phys. Rev. Lett.* **85** 2128
- [39] Honda M 2008 Phase-Transient Hierarchical Turbulence as an Energy Correlation Generator of Blazar Light Curves *Astrophys. J.* **675** L61
- [40] Chandrasekhar S and Kendall P C 1957 On Force-Free

- Magnetic Fields *Astrophys. J.* **126** 457
- [41] Schwinger J 1948 On Quantum-Electrodynamics and the Magnetic Moment of the Electron *Phys. Rev.* **73** 416
- [42] Witten E 1995 String Theory Dynamics in Various Dimensions *Nucl. Phys. B* **443** 85
- [43] Kaluza Th 1921 Zum Unitätsproblem der Physik *Sitzungsber. Preuss. Akad. Wiss. Berlin (Math. Phys.)* p 966
- [44] Klein O 1926 Quantentheorie und fünfdimensionale Relativitätstheorie *Zeit. f. Phys.* **37** 895
- [45] Particle Data Group Tanabashi M *et al* 2018 Review of Particle Physics *Phys. Rev. D* **98** 030001
- [46] The ATLAS and CMS Collaborations Aad G *et al* 2015 Combined Measurement of the Higgs Boson Mass in pp Collisions at $\sqrt{s} = 7$ and 8 TeV with the ATLAS and CMS Experiments *Phys. Rev. Lett.* **114** 191803
- [47] Gell-Mann M, Oakes R J and Renner B 1968 Behavior of Current Divergences under $SU_3 \times SU_3$ *Phys. Rev.* **175** 2195
- [48] KATRIN Collaboration Aker M *et al* 2019 Improved Upper Limit on the Neutrino Mass from a Direct Kinematic Method by KATRIN *Phys. Rev. Lett.* **123** 221802
- [49] Esfahani A A *et al* 2017 Determining the Neutrino Mass with Cyclotron Radiation Emission Spectroscopy – Project 8 *J. Phys. G: Nucl. Part. Phys.* **44** 054004
- [50] Pauli W Jr 1925 Über den Einfluß der Geschwindigkeitsabhängigkeit der Elektronenmasse auf den Zeemaneffekt *Zeit. f. Phys.* **31** 373
- [51] Pauli W Jr 1925 Über den Zusammenhang des Abschlusses der Elektronengruppen im Atom mit der Komplexstruktur der Spektren *Zeit. f. Phys.* **31** 765